Journal Pre-proof

A novel hydrogel-based treatment for complete transection spinal cord injury repair is driven by microglia/macrophages repopulation

Dezun Ma, Yannan Zhao, Lei Huang, Zhifeng Xiao, Bing Chen, Ya Shi, He Shen, Jianwu Dai

PII: S0142-9612(20)30076-4

DOI: https://doi.org/10.1016/j.biomaterials.2020.119830

Reference: JBMT 119830

To appear in: *Biomaterials*

Received Date: 7 July 2019

Revised Date: 28 December 2019

Accepted Date: 25 January 2020

Please cite this article as: Ma D, Zhao Y, Huang L, Xiao Z, Chen B, Shi Y, Shen H, Dai J, A novel hydrogel-based treatment for complete transection spinal cord injury repair is driven by microglia/macrophages repopulation, *Biomaterials* (2020), doi: https://doi.org/10.1016/j.biomaterials.2020.119830.

A Novel Hydrogel-based Treatment for Complete Transection Spinal Cord Injury Repair is Driven by Microglia/Macrophages Repopulation

Dezun Ma[a,b], Yannan Zhao[a] , Lei Huang[c] , Zhifeng Xiao[a] , Bing Chen[a] , Ya Shi[a], He Shen[c,]*, Jianwu Dai[a,b,*]

[a] State Key Laboratory of Molecular Developmental Biology, Institute of Genetics and Developmental Biology, Chinese Academy of Sciences, Beijing 100101, P.R. China.

[b] University of Chinese Academy of Sciences, Beijing, 100101, P.R. China

[c] Key Laboratory for Nano-Bio Interface Research, Division of Nanobiomedicine, Suzhou Institute of Nano-Tech and Nano-Bionics, Chinese Academy of Sciences, Suzhou 215123, China

Corresponding authors: Jianwu Dai, Email: jwdai@genetics.ac.cn

He Shen, Email: hshen2009@sinano.ac.cn

Acknowledgement

This work was supported by grants from the National Natural Science Foundation of China (No. 81891002, 81891003, 81971178), the Strategic Priority Research Program of the Chinese Academy of Sciences (No. XDA16040700) and the National Key Research and Development Program of China (2016YFC1101501, 2016YFC1101502, 2017YFA0104701, 2017YFA0104704).

Abstract

Microglia/macrophage mediated-inflammation, a main contributor to the microenvironment after spinal cord injury (SCI), persists for a long period of time and inhibits SCI repair. However, the effects of microglia/macrophage mediated-inflammation on neurogenic differentiation of endogenous neural stem/progenitor cells (NSPCs) are not well understood. In this study, to attenuate activated microglia/macrophage mediated-inflammation in the spinal cord of complete transection SCI mice, a combination of photo-crosslinked hydrogel transplantation and CSF1R inhibitor (PLX3397) treatment was used to replace the prolonged, activated microglia/macrophages via cell depletion and repopulation. This combined treatment in SCI mice produced a significant reduction in CD68-positive reactive microglia/macrophages and mRNA levels of pro-inflammatory factors, and a substantial increase in the number of Tuj1-positive neurons in the lesion area compared with single treatment methods. Moreover, most of the newborn Tuj1-positive neurons were confirmed to be generated from endogenous NSPCs using a genetic fate mapping mouse line (Nestin-CreERT2;LSL-tdTomato) that can label and trace NSPC marker-nestin expressing cells and their progenies. Collectively, our findings show that the combined treatment method for inhibiting microglia/macrophage mediated-inflammation promotes endogenous NSPC neurogenesis and improves functional recovery, which provides a promising therapeutic strategy for complete transection SCI.

Keywords: photo-crosslinked gelatin hydrogel, microglia/macrophages, inflammation, neurogenesis, complete transection spinal cord injury (SCI)

1. Introduction

Spinal cord injury (SCI) causes complex protracted neuroinflammation in the lesion epicenter and surrounding regions of the spinal cord, which contribute to the chronicity of tissue damage [1-4]. However, the spinal cord has "immune privilege" and a lack of lymphatic drainage making it hard to resolve inflammation [5]. The resolution of inflammation requires a purge of inflammatory cells and a reduction of pro-inflammation factors [6, 7]. Infiltrated polymorph-nuclear leucocytes (PMNs) and T lymphocytes can be cleared 14 days post SCI, however, activated microglia/macrophages can persist for a long time and contribute to prolonged inflammation [6, 8, 9]. In the SCI microenvironment, the morphological and immunological phenotypes of activated microglia/macrophages are difficult to return to the naïve state. Additionally, activated microglia/macrophages exist distal to the lesion and produce inflammatory mediators, thereby inhibiting spinal cord repair and homeostasis [6, 8, 10-13]. It has been well demonstrated that activated microglia/macrophage mediated-inflammation of the injured brain microenvironment not only impairs basal neurogenesis but also inhibits increased neurogenesis via activated microglia/macrophages and pro-inflammatory factors, such as tumor necrosis factor α (TNFα), interleukin 6 (IL6), and interferon γ (IFNγ) [14-19]. However, it is not clear whether microglia/macrophage mediated-inflammation inhibits neurogenesis and affects repair after severe SCI.

Gelatin, a denatured form of collagen, is considered an attractive alternative to native collagen (a major extracellular matrix component) as a biomaterial for tissue

engineering. A visible light (VL)–photo-crosslinked gelatin 3D hydrogel system with excellent biocompatibility and biodegradability has been developed that requires relatively mild chemical conditions, and has fast photoactivation and *in situ* formation [20, 21]. In addition, implanted gelatin sponges and gelatin-coated needles attenuated inflammation and reduced pro-inflammatory microglial/macrophage activation after SCI and brain injury, respectively [22, 23]. A three-dimensional (3D) gelatin sponge reduced the numbers of CD68-positive microglia/macrophages at the injured site, but not in surrounding tissue after SCI [24]. Although gelatin scaffolds effectively suppress activated microglia/macrophages after acute SCI or brain injury, they may only restrict in the lesion core, lack target specificity, and be unable to change the morphology of abnormal activated microglia/macrophages. Single transplantation of gelatin scaffolds may be not sufficient to resolve microglial/macrophage mediated-inflammation. Therefore, a new combined treatment strategy for efficiently resolving excessive activated microglial/macrophagemediated-inflammation is necessary.

Activated microglia/macrophages in traumatic brain-injured mice can be replaced with surveillant microglia via microglial elimination by PLX3397, a colony stimulating factor 1 receptor (CSF1R) inhibitor, followed by microglial repopulation. This treatment resolved the ongoing inflammation caused by the brain injury [25, 26]. This strategy provides an unprecedented cell replacement therapy for excessive activated microglia/macrophages and for manipulating microglial/macrophage morphology throughout the spinal cord, as well as for enhancing the effect of gelatin

hydrogel on reducing neuroinflammation.

In this study, we combined gelatin hydrogel transplantation with PLX3397 treatment to resolve microglia/macrophage mediated-inflammation after SCI. The number of activated microglia/macrophages was significantly reduced by the combined treatment of hydrogel transplantation and PLX3397 after complete transection SCI. The levels of pro-inflammatory factors also decreased dramatically with this combination treatment. Interestingly, we found that a large number of endogenous NSPCs differentiated into Tuj1-positive neurons with PLX3397 treatment and gelatin hydrogel implantation after SCI, and electrophysiological parameters and locomotion were significantly improved during recovery. Taken together, our results show that remodeling the microglia/macrophage mediated-inflammation microenvironment relieved inhibition of NSPC neurogenesis and enhanced regeneration effects.

2. Materials and methods

2.1 Animal Treatments

C57BL/6 mice were used. Nestin-CreER^{T2} (Stock No: 016261) and LSL-tdTomato (Stock No: 007909) mice were purchased from Jackson Laboratories (Port barrack, Maine, USA). Complete transection SCI mice were prepared according to our previous study [27]. Briefly, 1 mm of T7-T8 spinal cord tissue was removed after sodium pentobarbital (35 mg/kg) anesthesia. All animal husbandry and experiments were approved by the Institutional Animal Care and Use Committee of

the Chinese Academy of Sciences.

2.2 Synthesis and Characterization of Gelatin Hydrogel

The gelatin powder (Sigma) was derived from porcine skin with Vetec™ reagent grade. Preparation of methacrylated gelatin and the visible-light sensitive initiator, lithium phenyl-2,4,6-trimethylbenzoylphosphinate (LAP), as well as fabrication of gelatin hydrogel followed previously published instructions [20, 21, 28]. After photo-crosslinking 6% (w/v) methacrylated gelatin (containing 0.02% (w/v) LAP), the hydrogels were freeze-dried and the coated with gold. The micromorphology of the gelatin hydrogel was observed by SEM (Thermo Scientific™ Quanta™ SEM 400FEG, FEI Company) at 30.00 kV. Seventy scaffold pores were measured to analyze pore diameter. The compressive stress and modulus were measured using an Instron 5943 electromechanical universal testing machine (Instron Inc., USA). The swelling ratio of the hydrogel were calculated in accord with previous study [29].

2.3 Drug Administrations

PLX3397 was purchased from Plexxikon (USA) and added to AIN-76A chow (Research Diets) at 290 mg per kilogram. For nestin-expressing stem/progenitor cell lineage tracing, Nestin-CreER^{T2} mice were intraperitoneally injected with tamoxifen (Sigma) dissolved in corn oil (Sigma) (135 mg/kg) on 4 consecutive days before SCI surgery.

2.4 Immunofluorescence Staining and Imaging

Animals were perfused intracardially with cold 4% paraformaldehyde (PFA) in

phosphate buffered saline (PBS). Spinal cord tissues were collected, immersion-fixed in 4% PFA overnight at 4°C, cryo-protected in 30% sucrose, embedded in Tissue-Tek® O.C.T compound (Sakura) at -80°C, and then sectioned using a Leica CM1950 cryostat (Leica). The spinal cord sections were incubated with primary antibodies at 4°C overnight, followed by three washes with 1 × PBS and then incubated with secondary antibodies (1:500, Alexa Fluor 488 or Alexa Fluor 568, Invitrogen) for 2 hours at room temperature. The primary antibodies used were: rabbit anti-Iba1 (1:500, Wako, 019-19741), chicken anti-GFAP (1:1000, ab4674, Abcam), rabbit anti-NeuN (1:500, ab17748, Abcam), rabbit anti-Oligo2 (1:500, ab109186, Abcam), rat anti-CD68 (1:300, MCA1957, Bio-Rad), rabbit anti-Tuj1 (1:500, GTX130245, GeneTex), and rat anti-RFP (1:500, 5f8, ChromoTek). The spinal cord sections were imaged using a Leica SP8 confocal microscope.

2.5 Evans Blue Analysis

Two-month-old mice were intraperitoneally injected (4 mL/kg) with 2% (w/v) Evans Blue (Sigma) dissolved in 1×PBS, 6 hours before euthanasia. Spinal cords, spleens, livers, hearts, lungs, and kidneys were collected and incubated in 1 mL formamide for 24 hours at 55°C. The supernatant was collected and absorbance measured at 595 nm by a microplate reader (SpectraMax Plus 384, Molecular Devices).

2.6 Quantitative Real-Time PCR (qRT-PCR)

The mRNA levels of pro-inflammatory factors were measured by qRT-PCR.

Spinal cord tissues were harvested and total RNA extracted using Trizol (Invitrogen). cDNA was synthesized from total RNA by reverse transcription using a 1st Strand cDNA Synthesis SuperMix for qPCR (11123ES10, Yeasen). qRT-PCR was performed using SYBR Green Master Mix (A25742, Applied Biosystems) and a CFX96 Real-time system (Bio-Rad). Previously published primer sequences were used for all pro-inflammatory factors (**Table S1**) [30, 31].

2.7 Flow Cytometry

Whole blood (1.5 mL) was mixed with 3.8% sodium citrate (Beijing Chemical Work) at a 1:10 ratio. An equal volume of 1×PBS (Hycoll) was then added and mixed and then 5 mL Ficoll (Life Sciences) was added and the mixture centrifuged to collect the supernatant. The interface of the solutions was collected and washed with PBS three times. The spleen was triturated and washed with 1×PBS. Then, 2 mL red blood cell lysis buffer (40401ES60, Yeasen) was added and incubated for 5 minutes at room temperature. The antibodies used for staining were: APC-CD3 (Biolegend, 100236), PE-CD4 (BD biosciences, 3217924), FITC-CD8 (Biolegend, 100706), APC-CD19 (Biolegend, B240787), APC-Cy7–CD11b (Biolegend, 101226), PE-F4/80 (Biolegend, B262795), ACP-Ly6c (Biolegend, B234315), and PerCP-Cy5.5-MHCII (Biolegend, B253463). All samples were analyzed on a Life Technologies Attune NxT flow cytometer.

2.8 Functional Analysis

The Basso Mouse Scale (BMS) was used to evaluate the functional recovery of

SCI mice with or without treatment. Animals were assessed for hindlimb function every week by two independent observers. After treating SCI mice for 60 days, motor-evoked potentials were examined. Two stimulating electrodes were inserted onto the skull surface above the motor cortex. The recording electrodes were placed on the gastrocnemius muscle of the contralateral hindlimb to record after simulation at 45 mA.

2.9 Quantitative analyses

The region of interest (ROI) for quantification of Iba1 positive cells and Olig2 positive cells were measured within the entire cross-section of the spinal cord. The ROIs for quantification of NeuN positive cells were measured within the gray matter of the spinal cord. The ROIs for quantification of Iba1, CD68 positive cells were measured in the region 1 mm rostral and caudal to the lesion epicenter. The ROI for quantification of Tuj1, tdTomato positive cells was measured within the lesion epicenter of the spinal cord. The outline of the lesion epicenter was delineated by GFAP-staining, because the lesion area was surrounded by GFAP-positive astrocytes [32, 33]. The total numbers of immunolabeled cells in the ROI per section were counted in series with a random 147 um × 147 um counting frame. Cell bodies were only counted if they were located entirely within the counting frame. The cell density was represented as the average number of immunolabeled cells per mm^2 per section, calculated by the total number of cells in the entire counting frame divided by the area of the entire counting frame. An average of 300 counting frames were obtained from 9–12 sections from three to five mice per group. The mean gray values of GFAP

staining were measured within the entire transection of spinal cord in arbitrary units (A.U.). The optical density of Tuj1-stainning per section was measured in series in a random 147 um × 147 um box of the lesion area of the spinal cord. ImageJ software was used to measure the cell number and fluorescence intensity, and to delineate ROIs in each section.

3.0 Statistical Analysis

The data are presented as the mean ± standard deviation. Statistical analyses were performed with a one-way analysis of variance (ANOVA) followed by Tukey's post hoc test. All statistical analyses were performed using GraphPad, SPSS and Imaris 9.0.1. *, ** and *** are used to indicate $P<0.05$, $P<0.01$ and $P<0.001$, respectively.

3. Results

3.1 Characterization of Photo-crosslinked Gelatin Hydrogel

Implantation of gelatin sponges into SCI lesion sites can reduce the inflammatory response because fewer CD68-positive microglia/macrophages reside within the scaffold compared with the surrounding tissues [24]. In this study, gelatin hydrogels were formed *in situ* in the cavity of the injured spinal cord (**Fig. S1**). The morphology of the photo-crosslinked gelatin hydrogel was observed by scanning electron microscopy (SEM). As shown in **Fig. 1A** and **B**, freeze-dried hydrogel has a porous structure with holes ranging from 20 μm to 200 μm in diameter. The

compressive stress-strain curve of the gelatin hydrogel is shown in **Fig. 1C**, which is a typical curve for hydrogel scaffolds [34]. The compressive modulus of the gelatin hydrogel was 0.13±0.03 MPa, which is suitable for central nervous system (CNS) tissue engineering (**Fig. 1D**) [35]. The swelling ratio of the gelatin hydrogel was approximately 9.71 ± 1.04. After treating with gelatin hydrogel for 7 days, the NSPCs exhibited no obvious differences, indicating good biocompatibility of the scaffold (**Figure S2**).

3.2 Microglial Depletion and Repopulation in Uninjured Spinal Cord

To specifically regulate microglia/macrophages, PLX3397 was used to block CSF1R and to eliminate microglia from the spinal cord. After withdrawal of PLX3397, residual microglia repopulate the CNS via a self-renewal process. PLX3397 administration produces no obvious side effects or inflammatory responses in healthy mice [36, 37]. To confirm depletion and then repopulation of microglia in integrated spinal cord, we first examined microglial fate by feeding mice with a chow diet containing PLX3397. Approximately 26% and >80% of microglia were eliminated from the spinal cord after PLX3397 treatment for 7 days and 14 days, respectively (**Fig. 2A** and **C**). After stopping PLX3397 administration on the 14th day, the microglial repopulation occurred at 1 day and the number of residual microglia recovered to pre-administration levels over the next 14 days (**Fig. 2B** and **D, Fig S3**). To examine whether microglial depletion and subsequent repopulation affected other main cell types in the spinal cord, we immunohistochemically stained neurons, astrocytes and oligodendrocytes for NeuN, GFAP and Olig2, respectively. As shown

in Fig. 3A–E, the numbers of neurons and oligodendrocytes, and the fluorescence intensity of astrocytes displayed no difference among the healthy wild-type (WT) group, the microglial depletion (MD) group and the microglial repopulation (MP) group. In addition, there was no change in leukocyte populations in blood and spleen after PLX3397 microglial depletion (**Fig. S4–S9**). These results indicate that PLX3397 treatment is an effective pharmacological method to eliminate microglia that has few side effects on neural and glial cells and that does not alter the numbers of peripheral immune cells to disturb circulating immunity.

Next, to examine whether peripheral leukocytes invade the spinal cord after PLX3397-induced microglia depletion and repopulation in uninjured spinal cord, we examined the integrity of the blood-spinal cord barrier (BSCB) using Evans blue dye. The BSCB acts as a barrier to prohibit infiltration of peripheral immune cells and to maintain the immune-privileged milieu of the spinal cord. Evans blue dye binds to albumin and enters the spinal cord when the BSCB is disturbed [38]. There was no difference in Evans blue dye absorption in the spinal cord, liver, spleen, lung and kidney among WT, MD and MP groups (**Fig. S10).** These results demonstrate that the BSCB was not compromised after PLX3397 treatment. We then examined pro-inflammatory factors in the spinal cord by real-time quantitative PCR to confirm the safety of PLX3397. We found that mRNA levels of pro-inflammation factors, including IL1β, IL6, TNFα, iNOS, IFNγ and CCL2, were not altered in the MD and MP groups after microglial depletion compared with the WT group (**Fig. 5F–K** and **S11**). Taken together, these data demonstrate that use of the CSF1R inhibitor,

PLX3397, is a safe, effective pharmacological approach to specifically manipulate microglia/macrophages without impacting the inflammatory microenvironment of the spinal cord or altering peripheral leukocytes or other cell types in the spinal cord.

3.3 Morphological Evaluation of Repopulated Microglia/Macrophages after PLX3397 Treatment and Hydrogel Transplantation in Complete Transection SCI Mice

Having determined that PLX3397 caused no obvious effects on inflammatory responses or BSCB integrity in healthy mice, we modulated microglia/macrophages in SCI mice by treating with PLX3397 for 14 days (**Fig. 4A**). PLX3397 treatment [microglial depletion and repopulation (MDR) and MDR+Gelatin groups] significantly lowered the numbers of microglia/macrophages in SCI mice compared with the Gelatin and Control groups at day 14 post-surgery (**Fig. 4B–D**). After withdrawal of PLX3397 at day 14, the numbers of microglia/macrophages in both the MDR and MDR+Gelatin groups were recovered at day 60 post-surgery ($P<0.001$) (**Fig. 4D** and **E**). These results indicate that microglia/macrophages in the injured spinal cord can be depleted and repopulated by PLX3397 treatment.

After CNS injury, microglia/macrophages switch from having a long, ramified morphology to a hypertrophic or bushy cellular morphology that varies depending on the degree of injury and the time after injury (**Fig. 4F**) [39]. Microglia/macrophage phenotypes are closely related to the efficiency of SCI repair. For example, newborn neurons are removed by unchallenged microglial phagocytosis in the subgranular zone, thus harming neurogenesis [40]. Hence, we calculated the numbers of resting, hypertrophic and bushy Iba1-positive cells from the lesion to 1 mm distal to the lesion

279 to evaluate prolonged activated microglia/macrophage mediated-inflammation on the
280 60^{th} day post-surgery. As shown in **Fig. 4G** and **H**, transplanted gelatin hydrogel
281 reduced the proportion of microglia/macrophages with hypertrophic and bushy
282 morphologies compared with the control group, indicating its effect on attenuating
283 inflammation after SCI. Correspondingly, the MDR+Gelatin and MDR groups
284 exhibited substantially fewer hypertrophic or bushy Iba1-positive
285 microglia/macrophages compared with the Gelatin and Control groups (**Fig. 4G**–**J**).
286 These results indicate that transplantation of gelatin hydrogel in combination with
287 PLX3397 treatment is an effective strategy to revert dysfunctional microglia to
288 normal ones.

289 *3.4 Microglial/Macrophage Depletion and Repopulation in Combination with Gelatin*
290 *Hydrogel Transplantation Resolves Inflammation*

291 It is well established that prolonged activation of microglia/macrophages not
292 only changes their morphology but also causes expression of CD68 (a reactive
293 microglia/macrophage marker) and production of inflammatory factors in SCI models
294 [4]. To further assess the number of reactive microglia/macrophages, the number of
295 CD68-positive cells in the region 1 mm rostral and caudal to the lesion epicenter was
296 quantified. This measure is often used to evaluate microglia/macrophage
297 mediated-inflammation after SCI [41]. As shown in **Fig. 5A–C** and **E**, the Gelatin
298 group and the MDR group had fewer CD68-positive reactive microglia/macrophages
299 compared with the Control group 60 days after SCI ($P<0.01$). Compared to SCI mice
300 with gelatin hydrogel implantation or PLX3397 treatment, SCI mice with combined

treatment displayed a significant reduction in the number of CD68-positive microglia/macrophages ($p<0.001$) (**Fig. 5D** and **E**). In addition, reactive microglia/macrophages secrete numerous pro-inflammatory factors after CNS injury to regulate inflammation. Hence, we quantified mRNA levels of the pro-inflammation factors, IL1β, IL6, TNFα, iNOS, IFNγ and CCL2, to estimate microglia/macrophage mediated-inflammation responses. The expression of all pro-inflammatory cytokines was increased 60 days after SCI, demonstrating long-term inflammation (**Fig. 5F–K**). Transplantation of gelatin hydrogel slightly reduced the expression levels of pro-inflammatory factors, however, the iNOS expression level was significantly different between the Gelatin and the Control group (**Fig. 5J**). Moreover, the mRNA levels of IL1β, IL6, iNOS, IFNγ and CCL2 were also decreased in the MDR group compared with the Control group ($P<0.05$). The expression level of all six pro-inflammatory cytokines declined dramatically in the MDR+Gelatin combination treatment group ($P<0.01$) compared with any single therapy method (Gelatin and MDR groups), which was consistent with the CD68 immunohistochemical staining results (**Fig. 5F–K**). We also measured the levels of all pro-inflammatory factors at an early stage after SCI with or without treatment. At day 14 post-surgery, the mRNA levels of the pro-inflammatory cytokines were substantially decreased in the combined treatment group (MDR+Gelatin), indicating resolution of pro-inflammatory reactions after acute SCI (**Fig. S11**). These results demonstrated that combined treatment can resolve microglia/macrophage mediated acute and chronic pro-inflammation after SCI.

In this study, we first used a combination treatment to resolve microglia/macrophage mediated-inflammation at the lesion site and surrounding areas after complete transection SCI. By examining morphological shift, pro-inflammatory factor secretion and CD68 staining, we showed that the combined treatment more effectively resolved inflammation induced by microglia/macrophages compared with single therapies.

3.5 Microglial/Macrophage Depletion and Repopulation in Combination with Gelatin Hydrogel Transplantation Promotes Endogenous Neural Stem/Progenitor Cell Migration and Neurogenesis

In this study, to examine whether microglia/macrophage mediated-inflammation affects endogenous neurogenesis, we visualized newborn neurons by immunohistochemical staining of neuronal class III β-tubulin (Tuj1) in the lesion area after complete transection SCI. As shown in **Fig. 6A** and **B**, the numbers of Tuj1-positive neurons in the lesion area increased with transplantation of gelatin hydrogels or PLX3397 treatment compared with the control at 60 days after surgery ($p<0.001$). More importantly, the MDR+Gelatin group had a significantly higher number of Tuj1-positive neurons in the SCI lesion site compared with the other three groups ($p<0.001$). These results indicate that microglial/macrophage mediated-inflammation restricts the generation of newborn neurons after complete transection SCI, and that modulating the inflammatory microenvironment by the combined treatment method accelerated neural regeneration.

Nestin, a NSPC marker, is expressed in ependymal cells of adult spinal cord [42].

We speculate that the Tuj1-positive cells in the lesion area were generated from nestin-expressing NSPCs. To accurately test this assumption, we used Nestin-CreER^{T2} driver mice, in which nestin-positive cells express CreER, and crossed them with the Rosa-stop-tdTomato reporter mouse line. In the Nestin-CreER^{T2};LSL-tdTomato mouse, nestin-expressing cells and their progenies are labeled and can be traced after tamoxifen induction (**Fig. 6C**). All nestin-expressing cells and their progenies were labeled red after tamoxifen induction (**Fig. 6D**). We treated Nestin-CreER^{T2};LSL-tdTomato mice with tamoxifen based on body weight (135 mg/g) for 5 days prior to SCI to permanently label nestin-expressing NSPCs. Many more tdTomato-positive cells migrated to the lesion area and differentiated into Tuj1-positive neurons in the complete transection SCI mice treated with both hydrogel transplantation and PLX3397 compared with single treatment mice (Gelatin or MDR groups) ($P<0.001$) (**Fig. 6E–G**). Although single therapies exhibited less neurogenesis than the combination treatment, the number of Tuj1-positive neurons in the Gelatin and MDR groups also increased compared with the Control group ($P<0.001$). Collectively, we found that resolution of microglia/macrophage mediated-inflammation by the combined treatment promoted endogenous NSPC migration and neurogenic differentiation.

3.6 Microglial/Macrophage Modulation in Combination with Hydrogel Transplantation Improves Electrophysiological and Functional Recovery of Transected SCI Mice

At 60 days post injury, the motor function of the four groups was assessed by

367 determining Basso Mouse Scale (BMS) scores. **Fig. 7**A shows that MDR+Gelatin
368 group scores from five weeks to eight weeks were significantly higher compared with
369 those of the Control group ($P<0.05$). At 8 weeks, the score of the MDR+Gelatin group
370 (2.9±0.7) was much higher than that of the Control (1.2±0.7), Gelatin (2.3±0.8) and
371 MDR (2.5±1.0) groups, indicating more efficient functional recovery. To further
372 estimate the level of functional recovery, we performed electrophysiological analyses.
373 The amplitude of the Control group was much lower than that of healthy mice. The
374 amplitudes in the single treatment groups (Gelatin and MDR groups) were
375 substantially increased compared with the Control group ($p<0.001$). More importantly,
376 the amplitude was partly restored in the MDR+Gelatin group, and was the highest
377 among the four groups ($p<0.001$) (**Fig. 7B** and **C**). These results showed that
378 locomotor function could recover in complete transection SCI mice after combined
379 PLX3397 and hydrogel transplantation treatment.

380 **4. Discussion**

381 Spinal cord injury (SCI) appears following primary mechanical damage and a
382 series of secondary insults. Neuro-inflammation, glial scar formation, and neurite
383 growth-inhibitory factor accumulation can exacerbate injured and intact tissue,
384 resulting in movement and/or sensatory deficits below the lesion site [43, 44]. Such
385 lesions are currently a major clinical challenge for SCI repair [44]. Stem cell-based
386 therapy for SCI repair provides a promising clinical strategy for bridging the lesion
387 and promoting regeneration of neurons, axons and glia [45-47]. Transplanted stem
388 cells not only differentiate into neurons and oligodendrocytes to replenish lost cells,

but also secrete neurotrophic and growth factors to promote endogenous regeneration, synapse formation and remyelination [48]. In addition, biomaterial-based matrices could also fill the lesion gap and create a permissive environment and structure to support axonal regeneration and functional reconnection [49-52]. However, the inflammatory response after SCI may affect the therapeutic efficiency of biomaterial and stem cell transplantation. Hence, it may be useful to develop a method for resolving inflammatory responses in combination with the transplantation of biomaterials or stem cells. Microglia are the primary resident immune cells of the CNS and play a critical role after injury [53]. After spinal cord injury, protracted inflammation is mainly induced by amoeboid and phagocytic macrophages that are generated from rapidly activated microglia and peripheral macrophages [54]. Unlike other immune cells that accumulate in lesions post SCI, prolonged activated microglia/macrophages persist for a longer period and participate in secondary damage [8, 12, 13]. Although microglia/macrophages are crucial to the inflammatory microenvironment and functional recovery after SCI, it is difficult to selectively resolve activated microglia/macrophage mediated-persistent inflammation. These difficulties can be divided into three categories: i) activated microglia/macrophages may not be restricted to a lesion epicenter, but may also be activated in remote areas and produce inflammatory factors [4]. For instance, after SCI, activated microglia/macrophages were observed in the brain [11]. However, transplanted scaffolds and anti-inflammation drugs delivered by biomaterial-based carriers mainly remained and worked in lesion sites, while the protracted activated

411 microglia/macrophages in remote areas are unaffected. ii) In addition to the secretion
412 of inflammatory factors, the morphology of protracted, activated
413 microglia/macrophages also changed; the cell bodies appeared large with short
414 dysfunctional process. Although many strategies can inhibit activation and
415 proliferation of microglia/macrophages, it is hard to replace dysfunctional activated
416 microglia/macrophages with functional microglia. iii) It is difficult to specifically
417 manipulate microglia/macrophages without affecting other neural or immune cells.
418 Hence, because of these issues it is necessary to develop a new strategy to resolve
419 microglia/macrophage mediated-inflammation.

420 In this study, we applied a novel combined treatment to resolve
421 microglia/macrophage mediated-persistent inflammation. This combined treatment
422 consisted of transplanted photocrosslinkable gelatin hydrogel to the lesion site
423 combined with fed a CSF1R inhibitor, PLX3397 for SCI mice. Implantation of gelatin
424 sponges into SCI lesion sites can reduce the inflammatory response because fewer
425 CD68-positive microglia/macrophages reside within the scaffold compared with the
426 surrounding tissues [24]. A hybrid gelatin porous scaffold impregnated with fucoidan
427 and sodium alginate suppressed the lipopolysaccharide (LPS)-induced inflammation
428 in cultured microglial cells [55]. Recently, PLX3397 has been widely used to
429 investigate the role of microglia in the central nervous system (CNS). Inhibition of
430 CSF1R by PLX3397 rapidly eliminated microglia from mouse brain without any
431 detrimental effects on neurons or peripheral immune cells [36, 56]. Moreover,
432 PLX3397 reduced brain injury after intracerebral hemorrhage via microglia depletion

433 [57]. Gerber et al. also found that reducing microglial proliferation using a CSF1R
434 inhibitor promoted locomotor recovery after early spinal cord injury [58]. However,
435 as the main immune cells in the CNS, it is not feasible to clinically eliminate
436 microglia from humans. Hence, Rice et al. treated brain-injured mice with PLX3397
437 for 14 days and then withdrew PLX3397 and found that residual microglia
438 repopulated the whole brain. Interestingly, they found that newborn microglia had a
439 naïve state morphology and that persistent inflammation was resolved by this
440 treatment [25]. Here, we introduced a combined treatment to significantly improve the
441 efficiency of resolving microglia/macrophage mediated-inflammation compared with
442 single PLX3397 treatment or transplantation of hydrogel. Moreover, the combined
443 treatment largely resolved the microglia/macrophage mediated-inflammation in the
444 lesion site and surrounding tissue by reducing levels of CD68 protein and
445 pro-inflammatory factors without affecting the number of neurons, neuroglial cells or
446 immune cells in the blood and spleen. Furthermore, we also found that the proportion
447 of hypertrophic and bushy microglia/macrophages was decreased after combined
448 treatment in SCI mice. Together, these data demonstrated that this combined treatment
449 is a safe, extensive and high-effective method to resolve microglia/macrophage
450 mediated-inflammation.

451 Next we investigated the role of microglia/macrophage mediated-inflammation
452 in SCI mice by the combined treatment. It is well established that one of the biggest
453 challenges for repair of complete transection SCI is the loss of a large number of
454 neurons in the lesion area, resulting in functional deficiency [59]. Although many

attempts have been made to replenish this neuronal loss by transplanting NSPCs after SCI, immunological rejection, a lack of suitable NSPC sources and ethical concerns have limited the clinical application of cell transplantation [60]. Therefore, manipulating endogenous stem or progenitor cells to migrate and differentiate into neurons at the lesion area is an attractive proposition. Ependymal cells, which line the central canal of mammalian spinal cords, are considered as endogenous NSPCs [61]. After SCI, these ependymal cells can be activated and can proliferate to produce some benefit in SCI repair. However, few neurons differentiate from these endogenous NSPCs because of the inflammatory microenvironment, which limits the capacity for self-repair [62]. Microglia regulate neurogenesis by apoptosis-coupled phagocytosis in the hippocampus of adult mice [40]. In addition, Gomes-Leal reported that overactivated microglia inhibit neuroblast migration, but ramified microglia promote migration of immature neurons in the ventral striatum after middle cerebral artery occlusion [63]. Furthermore, activated microglia mediated-inflammation induced by lipopolysaccharide (LPS) injection or brain injury impairs neurogenesis in adult brain [14]. Although it is well known that microglia/macrophage mediated-inflammation is detrimental for neurogenesis after brain injury, it was unclear whether this was the case in spinal cord injury. Hence, we used the combined treatment to explore whether relieving microglia/macrophage mediated-inflammation affects NSPCs neurogenesis. Lineage tracing using Nestin-CreERT2;LSL-tdTomato mice showed that the large number of Tuj1-positive neurons that appeared in the SCI lesion area were generated from NPSCs after the combined treatment. This is the first demonstration that

477 microglia/macrophage mediated-inflammation inhibits newborn neurons generated
478 from NPSCs. Chen et al. claimed that a gelatin fiber scaffold was suitable for cell
479 migration and long-term survival, and promoted neural differentiation and inhibited
480 glia scar formation [64]. Gelatin (containing RGD peptides) has advantages for cell
481 adhesion [65, 66], which might benefit endogenous NSPC migration to the injured
482 site. In this study, the photo-crosslinked gelatin hydrogel not only attenuated
483 microglia/macrophage mediated-inflammation, but may have also served as a
484 substrate for cell growth, migration and differentiation, as well as acting as a bridge to
485 fill defect sites and for connecting damaged tissues. Hence, we suggest that the
486 modulated microenvironment in the MDR+Gelatin group had positive effects on both
487 resolving inflammation and guiding NSPC migration and neurogenesis. For potential
488 clinical application of this combination system (PLX3397 is a FDA approved drug),
489 the source of gelatin, the synthesis procedure, and storage should be standardized
490 according to the requirements for clinical trials. In addition, large animal models
491 provide a number of translational advantages [67], which should be used as tools for
492 ongoing clinical research. In the current study, we estimated the biocompatibility of
493 the hydrogel in vitro. The in vivo biosafety and biodegradation of the hydrogel will be
494 examined further in future research, and will also be evaluated by a third party.

495 When SCI occurs, activated microglia/macrophages release a mass of
496 pro-inflammatory cytokines and neurotoxic factors to accelerate the loss of neurons
497 and inhibit axon regrowth [68-70]. In addition, in the first week after SCI,
498 microglia/macrophages mediated-inflammation also contributes to the potential

hostile microenvironment that leads to rejection of transplanted neural stem cells for SCI repair [71]. Accumulating evidence indicates that attenuating activated microglia/macrophages by minocycline, an anti-inflammatory drug, facilitated neuroprotection and functional recovery after SCI [41, 72, 73]. Conversely, activated microglia/macrophages also play a beneficial neuroprotective role in SCI repair by secretion of anti-inflammatory factors and phagocytosis of injurious debris [74]. Hence, harnessing monocyte-derived macrophages to repair the damaged spinal cord is also a potential therapeutic strategy for SCI repair [75]. Transplantation of mesenchymal stem cells into the injured spinal cord could also involve recruitment of the M2 phenotype macrophage for SCI repair [76]. The heterogeneity of microglia/macrophages, which can be divided into M1 or M2 phenotypes, is a possible reason for their different functions in SCI. M1 microglia/macrophages are pro-inflammatory and cytotoxic, while M2 microglia/macrophages are anti-inflammatory and promote regeneration after SCI [10]. In addition, the effect of activated microglia/macrophages may change based on the progress of SCI. In acute SCI, activated microglia/macrophages are of mixed M1 and M2 phenotypes, but M1 phenotype microglia/macrophages persist for a long period of time [77]. This evidence suggests that the functions of microglia vary depending on the degree of injury, location, and timing in the SCI model. Here, the data indicate that combined treatment resolved microglia/macrophage-mediated persistent inflammation and ameliorated SCI progression. This combined treatment may alter the phenotype of prolonged activated microglia/macrophages in a cell replacement strategy, resolving

the microglia/macrophage-mediated inflammation in a persistent way. We also found that locomotor function of complete transection SCI mice recovered with combined treatment. These findings suggest that resolution of prolonged activated microglia/macrophage-mediated inflammation by combined treatment might produce a permissive microenvironment for neuronal survival, axon regeneration and neurogenic differentiation of NSPCs, thus promoting functional recovery after complete transection SCI.

As summarized in **Fig. 8**, a novel and effective combined treatment can resolve microglia/macrophage mediated-inflammation after complete transection SCI. Moreover, we demonstrate that relieving microglia/macrophage mediated-inflammation by this combined treatment promotes neurogenesis in SCI mice.

5. Conclusions

In this study, we explored the interaction between microglia/macrophage mediated-inflammation and neurogenesis following gelatin hydrogel transplantation in combination with CSF1R inhibitor (PLX3397) treatment after complete transection SCI. We found that microglia/macrophage mediated-inflammation inhibited the neurogenesis of endogenous NSPCs. Compared with transplantation of gelatin hydrogel or PLX3397 treatment single treatments, a combination of the two significantly resolved inflammation and enhanced generation of newborn neurons from endogenous NSPCs and, therefore, promoted recovery of locomotor function. In summary, we constructed a low inflammation microenvironment to improve

543 functional restoration in complete transection SCI mice via a safe, effective
544 combination treatment strategy, which has the potential to be clinically applied.
545

546 **Acknowledgements**

547 This work was supported by grants from the National Natural Science Foundation of
548 China (No. 81891002, 81891003 and 81971178), the Strategic Priority Research
549 Program of the Chinese Academy of Sciences (No. XDA16020100) and the National
550 Key Research and Development Program of China (2016YFC1101501,
551 2016YFC1101502, 2017YFA0104701 and 2017YFA0104704).
552

553 **Supporting Data**

554 Supplementary data includes nine Figures and one Table.
555

556 **Disclosure**

557 The authors declare no conflict of interest.
558

559 **Data availability statement**

560 The data are available from the corresponding author on reasonable request.
561
562

References

[1] J.K. Alexander, P.G. Popovich, Neuroinflammation in spinal cord injury: therapeutic targets for neuroprotection and regeneration, Progress in brain research. 175 (2009) 125-37.

[2] J. Silver, M.E. Schwab, P.G. Popovich, Central nervous system regenerative failure: role of oligodendrocytes, astrocytes, and microglia, Cold spring harbor perspectives in biology. 7(3) (2014) a020602.

[3] M.R. Detloff, L.C. Fisher, V. McGaughy, E.E. Longbrake, P.G. Popovich, D.M. Basso, Remote activation of microglia and pro-inflammatory cytokines predict the onset and severity of below-level neuropathic pain after spinal cord injury in rats, Experimental neurology. 212(2) (2008) 337-47.

[4] P. Zhao, S.G. Waxman, B.C. Hains, Modulation of thalamic nociceptive processing after spinal cord injury through remote activation of thalamic microglia by cysteine cysteine chemokine ligand 21, The Journal of neuroscience : the official journal of the society for neuroscience. 27(33) (2007) 8893-902.

[5] I. Galea, I. Bechmann, V.H. Perry, What is immune privilege (not)?, Trends in immunology. 28(1) (2007) 12-8.

[6] C.N. Serhan, S.D. Brain, C.D. Buckley, D.W. Gilroy, C. Haslett, L.A. O'Neill, M. Perretti, A.G. Rossi, J.L. Wallace, Resolution of inflammation: state of the art, definitions and terms, FASEB journal : official publication of the federation of american societies for experimental biology. 21(2) (2007) 325-32.

[7] D.W. Gilroy, T. Lawrence, M. Perretti, A.G. Rossi, Inflammatory resolution: new opportunities for drug discovery, Nature reviews drug discovery. 3(5) (2004) 401-16.

[8] H. Pruss, M.A. Kopp, B. Brommer, N. Gatzemeier, I. Laginha, U. Dirnagl, J.M. Schwab, Non-resolving aspects of acute inflammation after spinal cord injury (SCI): indices and resolution plateau, Brain pathology. 21(6) (2011) 652-60.

[9] T. Lawrence, D.W. Gilroy, Chronic inflammation: a failure of resolution?, International journal of experimental pathology. 88(2) (2007) 85-94.

[10] S. David, A. Kroner, Repertoire of microglial and macrophage responses after spinal cord injury, Nature reviews. Neuroscience. 12(7) (2011) 388-99.

[11] J. Wu, Z. Zhao, B. Sabirzhanov, B.A. Stoica, A. Kumar, T. Luo, J. Skovira, A.I. Faden, Spinal cord injury causes brain inflammation associated with cognitive and affective changes: role of cell cycle pathways, The Journal of neuroscience : the official journal of the society for neuroscience. 34(33) (2014) 10989-1006.

[12] H.M. Bramlett, W.D. Dietrich, Progressive damage after brain and spinal cord injury: pathomechanisms and treatment strategies, Progress in brain research. 161 (2007) 125-41.

[13] M.O. Totoiu, H.S. Keirstead, Spinal cord injury is accompanied by chronic progressive demyelination, The Journal of comparative neurology. 486(4) (2005) 373-83.

[14] C.T. Ekdahl, J.H. Claasen, S. Bonde, Z. Kokaia, O. Lindvall, Inflammation is detrimental for neurogenesis in adult brain, Proceedings of the national academy of sciences of the united states of america. 100(23) (2003) 13632-7.

[15] M.A. Curtis, M. Kam, U. Nannmark, M.F. Anderson, M.Z. Axell, C. Wikkelso, S. Holtas, W.M. van Roon-Mom, T. Bjork-Eriksson, C. Nordborg, J. Frisen, M. Dragunow, R.L. Faull, P.S. Eriksson, Human neuroblasts migrate to the olfactory bulb via a lateral ventricular extension, Science.

315(5816) (2007) 1243-9.
[16] A.D. Bachstetter, J.M. Morganti, J. Jernberg, A. Schlunk, S.H. Mitchell, K.W. Brewster, C.E. Hudson, M.J. Cole, J.K. Harrison, P.C. Bickford, C. Gemma, Fractalkine and CX 3 CR1 regulate hippocampal neurogenesis in adult and aged rats, Neurobiology of aging. 32(11) (2011) 2030-44.
[17] L. Vallieres, I.L. Campbell, F.H. Gage, P.E. Sawchenko, Reduced hippocampal neurogenesis in adult transgenic mice with chronic astrocytic production of interleukin-6, The Journal of neuroscience : the official journal of the society for neuroscience. 22(2) (2002) 486-92.
[18] T. Ben-Hur, O. Ben-Menachem, V. Furer, O. Einstein, R. Mizrachi-Kol, N. Grigoriadis, Effects of proinflammatory cytokines on the growth, fate, and motility of multipotential neural precursor cells, Molecular and cellular neurosciences. 24(3) (2003) 623-31.
[19] M.K. Tobin, J.A. Bonds, R.D. Minshall, D.A. Pelligrino, F.D. Testai, O. Lazarov, Neurogenesis and inflammation after ischemic stroke: what is known and where we go from here, Journal of cerebral blood flow and metabolism : official journal of the international society of cerebral blood flow and metabolism. 34(10) (2014) 1573-84.
[20] H. Lin, A.M. Beck, K. Shimomura, J. Sohn, M.R. Fritch, Y. Deng, E.J. Kilroy, Y. Tang, P.G. Alexander, R.S. Tuan, optimization of photocrosslinked gelatin/hyaluronic acid hybrid scaffold for the repair of cartilage defect, Journal of tissue engineering and regenerative medicine. 13(8) (2019) 1418-1429.
[21] H. Lin, A.W. Cheng, P.G. Alexander, A.M. Beck, R.S. Tuan, Cartilage tissue engineering application of injectable gelatin hydrogel with in situ visible-light-activated gelation capability in both air and aqueous solution, Tissue engineering. Part A. 20(17-18) (2014) 2402-11.
[22] L.S. Kumosa, V. Zetterberg, J. Schouenborg, Gelatin promotes rapid restoration of the blood brain barrier after acute brain injury, Acta biomaterialia. 65 (2018) 137-149.
[23] G. Lind, C.E. Linsmeier, J. Thelin, J. Schouenborg, Gelatine-embedded electrodes--a novel biocompatible vehicle allowing implantation of highly flexible microelectrodes, Journal of neural engineering. 7(4) (2010) 046005.
[24] X. Zeng, Y.S. Zeng, Y.H. Ma, L.Y. Lu, B.L. Du, W. Zhang, Y. Li, W.Y. Chan, Bone marrow mesenchymal stem cells in a three-dimensional gelatin sponge scaffold attenuate inflammation, promote angiogenesis, and reduce cavity formation in experimental spinal cord injury, Cell transplantation. 20(11-12) (2011) 1881-99.
[25] R.A. Rice, J. Pham, R.J. Lee, A.R. Najafi, B.L. West, K.N. Green, Microglial repopulation resolves inflammation and promotes brain recovery after injury, Glia. 65(6) (2017) 931-944.
[26] J. Han, K. Zhu, X.M. Zhang, R.A. Harris, Enforced microglial depletion and repopulation as a promising strategy for the treatment of neurological disorders, Glia. 67(2) (2019) 217-231.
[27] X. Li, S. Liu, Y. Zhao, J. Li, W. Ding, S. Han, B. Chen, Z. Xiao, J. Dai, Training neural stem cells on functional collagen scaffolds for severe spinal cord injury repair, Advanced functional materials. 26(32) (2016) 5835-5847.
[28] H. Shen, H. Lin, A.X. Sun, S.J. Song, Z.J. Zhang, J.W. Dai, R.S. Tuan, Chondroinductive factor-free chondrogenic differentiation of human mesenchymal stem cells in graphene oxide-incorporated hydrogels, Journal of materials chemistry b. 6(6) (2018) 908-917.
[29] H. Park, X. Guo, J.S. Temenoff, Y. Tabata, A.I. Caplan, F.K. Kasper, A.G. Mikos, Effect of swelling ratio of injectable hydrogel composites on chondrogenic differentiation of encapsulated rabbit marrow mesenchymal stem cells in vitro, Biomacromolecules. 10(3) (2009) 541-6.
[30] G. Liu, G. Fan, G. Guo, W. Kang, D. Wang, B. Xu, J. Zhao, FK506 Attenuates the inflammation

in rat spinal cord injury by inhibiting the activation of NF-kappaB in microglia cells, Cellular and molecular neurobiology. 37(5) (2017) 843-855.
[31] X. Yang, H. Ren, K. Wood, M. Li, S. Qiu, F.D. Shi, C. Ma, Q. Liu, Depletion of microglia augments the dopaminergic neurotoxicity of MPTP, FASEB journal : official publication of the federation of american societies for experimental biology. 32(6) (2018) 3336-3345.
[32] T.M. O'Shea, J.E. Burda, M.V. Sofroniew, Cell biology of spinal cord injury and repair, The Journal of clinical investigation. 127(9) (2017) 3259-3270.
[33] M.A. Anderson, J.E. Burda, Y. Ren, Y. Ao, T.M. O'Shea, R. Kawaguchi, G. Coppola, B.S. Khakh, T.J. Deming, M.V. Sofroniew, Astrocyte scar formation aids central nervous system axon regeneration, Nature. 532(7598) (2016) 195-200.
[34] E.M. Ahmed, Hydrogel: preparation, characterization, and applications: a review, Journal of advanced research. 6(2) (2015) 105-21.
[35] R.D. Bartlett, D. Choi, J.B. Phillips, Biomechanical properties of the spinal cord: implications for tissue engineering and clinical translation, Regenerative medicine. 11(7) (2016) 659-73.
[36] M.R. Elmore, A.R. Najafi, M.A. Koike, N.N. Dagher, E.E. Spangenberg, R.A. Rice, M. Kitazawa, B. Matusow, H. Nguyen, B.L. West, K.N. Green, Colony-stimulating factor 1 receptor signaling is necessary for microglia viability, unmasking a microglia progenitor cell in the adult brain, Neuron. 82(2) (2014) 380-97.
[37] Y. Huang, Z. Xu, S. Xiong, F. Sun, G. Qin, G. Hu, J. Wang, L. Zhao, Y.X. Liang, T. Wu, Z. Lu, M.S. Humayun, K.F. So, Y. Pan, N. Li, T.F. Yuan, Y. Rao, B. Peng, Repopulated microglia are solely derived from the proliferation of residual microglia after acute depletion, Nature neuroscience. 21(4) (2018) 530-540.
[38] M. Radu, J. Chernoff, An in vivo assay to test blood vessel permeability, Journal of visualized experiments : JoVE. (73) (2013) e50062.
[39] U.K. Hanisch, H. Kettenmann, Microglia: active sensor and versatile effector cells in the normal and pathologic brain, Nature neuroscience. 10(11) (2007) 1387-94.
[40] A. Sierra, J.M. Encinas, J.J. Deudero, J.H. Chancey, G. Enikolopov, L.S. Overstreet-Wadiche, S.E. Tsirka, M. Maletic-Savatic, Microglia shape adult hippocampal neurogenesis through apoptosis-coupled phagocytosis, Cell stem cell. 7(4) (2010) 483-95.
[41] Z. Wang, J. Nong, R.B. Shultz, Z. Zhang, T. Kim, V.J. Tom, R.K. Ponnappan, Y. Zhong, Local delivery of minocycline from metal ion-assisted self-assembled complexes promotes neuroprotection and functional recovery after spinal cord injury, Biomaterials. 112 (2017) 62-71.
[42] K. Liu, Z. Wang, H. Wang, Y. Zhang, Nestin expression and proliferation of ependymal cells in adult rat spinal cord after injury, Chinese medical journal. 115(3) (2002) 339-41.
[43] A.E. Mautes, M.R. Weinzierl, F. Donovan, L.J. Noble, Vascular events after spinal cord injury: contribution to secondary pathogenesis, Physical therapy. 80(7) (2000) 673-87.
[44] I.C. Maier, M.E. Schwab, Sprouting, regeneration and circuit formation in the injured spinal cord: factors and activity, Philosophical transactions of the royal society of london. Series B, Biological sciences. 361(1473) (2006) 1611-34.
[45] J. Ruzicka, L. Machova-Urdzikova, J. Gillick, T. Amemori, N. Romanyuk, K. Karova, K. Zaviskova, J. Dubisova, S. Kubinova, R. Murali, E. Sykova, M. Jhanwar-Uniyal, P. Jendelova, A comparative study of three different types of stem cells for treatment of rat spinal cord injury, Cell transplantation. 26(4) (2017) 585-603.
[46] D. Lukovic, V. Moreno-Manzano, E. Lopez-Mocholi, F.J. Rodriguez-Jimenez, P. Jendelova, E.

694 Sykova, M. Oria, M. Stojkovic, S. Erceg, Complete rat spinal cord transection as a faithful model of
695 spinal cord injury for translational cell transplantation, Scientific reports. 5 (2015) 9640.
696 [47] S. Estrada-Mondaca, A. Carreon-Rodriguez, C. Parra-Cid Mdel, C.I. Leon, C.
697 Velasquillo-Martinez, C.A. Vacanti, J. Belkind-Gerson, [Spinal cord injury and regenerative
698 medicine], Salud publica de mexico. 49(6) (2007) 437-44.
699 [48] A.P. Pego, S. Kubinova, D. Cizkova, I. Vanicky, F.M. Mar, M.M. Sousa, E. Sykova, Regenerative
700 medicine for the treatment of spinal cord injury: more than just promises?, Journal of cellular and
701 molecular medicine. 16(11) (2012) 2564-82.
702 [49] R. Langer, J. Vacanti, Advances in tissue engineering, Journal of pediatric surgery. 51(1) (2016)
703 8-12.
704 [50] M.P. Vacanti, J.L. Leonard, B. Dore, L.J. Bonassar, Y. Cao, S.J. Stachelek, J.P. Vacanti, F.
705 O'Connell, C.S. Yu, A.P. Farwell, C.A. Vacanti, Tissue-engineered spinal cord, Transplantation
706 proceedings. 33(1-2) (2001) 592-8.
707 [51] H. Park, C. Cannizzaro, G. Vunjak-Novakovic, R. Langer, C.A. Vacanti, O.C. Farokhzad,
708 Nanofabrication and microfabrication of functional materials for tissue engineering, Tissue
709 engineering. 13(8) (2007) 1867-77.
710 [52] A. Hejcl, P. Lesny, M. Pradny, J. Michalek, P. Jendelova, J. Stulik, E. Sykova, Biocompatible
711 hydrogels in spinal cord injury repair, Physiological research. 57 Suppl 3 (2008) S121-32.
712 [53] A. Nimmerjahn, F. Kirchhoff, F. Helmchen, Resting microglial cells are highly dynamic
713 surveillants of brain parenchyma in vivo, Science. 308(5726) (2005) 1314-8.
714 [54] G.W. Kreutzberg, Microglia: a sensor for pathological events in the CNS, Trends in
715 neurosciences. 19(8) (1996) 312-8.
716 [55] V.T. Nguyen, S.C. Ko, G.W. Oh, S.Y. Heo, Y.J. Jeon, W.S. Park, I.W. Choi, S.W. Choi, W.K. Jung,
717 Anti-inflammatory effects of sodium alginate/gelatine porous scaffolds merged with fucoidan in
718 murine microglial BV2 cells, International journal of biological macromolecules. 93(Pt B) (2016)
719 1620-1632.
720 [56] N.N. Dagher, A.R. Najafi, K.M. Kayala, M.R. Elmore, T.E. White, R. Medeiros, B.L. West, K.N.
721 Green, Colony-stimulating factor 1 receptor inhibition prevents microglial plaque association and
722 improves cognition in 3xTg-AD mice, Journal of neuroinflammation. 12 (2015) 139.
723 [57] M. Li, Z. Li, H. Ren, W.N. Jin, K. Wood, Q. Liu, K.N. Sheth, F.D. Shi, Colony stimulating factor 1
724 receptor inhibition eliminates microglia and attenuates brain injury after intracerebral
725 hemorrhage, Journal of cerebral blood flow and metabolism : official journal of the International
726 society of cerebral blood flow and metabolism. 37(7) (2017) 2383-2395.
727 [58] Y.N. Gerber, G.P. Saint-Martin, C.M. Bringuier, S. Bartolami, C. Goze-Bac, H.N. Noristani, F.E.
728 Perrin, CSF1R inhibition reduces microglia proliferation, promotes tissue preservation and
729 improves motor recovery after spinal cord injury, Frontiers in cellular neuroscience. 12 (2018)
730 368.
731 [59] J.W. McDonald, C. Sadowsky, Spinal-cord injury, Lancet. 359(9304) (2002) 417-25.
732 [60] A.J. Mothe, C.H. Tator, Review of transplantation of neural stem/progenitor cells for spinal
733 cord injury, International journal of developmental neuroscience : the official journal of the
734 international society for developmental neuroscience. 31(7) (2013) 701-13.
735 [61] K. Meletis, F. Barnabe-Heider, M. Carlen, E. Evergren, N. Tomilin, O. Shupliakov, J. Frisen,
736 Spinal cord injury reveals multilineage differentiation of ependymal cells, PLoS biology. 6(7) (2008)
737 e182.

[62] F. Barnabe-Heider, C. Goritz, H. Sabelstrom, H. Takebayashi, F.W. Pfrieger, K. Meletis, J. Frisen, Origin of new glial cells in intact and injured adult spinal cord, Cell stem cell. 7(4) (2010) 470-82.
[63] W. Gomes-Leal, Why microglia kill neurons after neural disorders? The friendly fire hypothesis, Neural regeneration research. 14(9) (2019) 1499-1502.
[64] C. Chen, J. Tang, Y. Gu, L. Liu, X. Liu, L. Deng, C. Martins, B. Sarmento, W. Cui, L. Chen, Bioinspired hydrogel electrospun fibers for spinal cord regeneration, Advanced functional materials. 29(4) (2019) 1806899.
[65] X. Li, J. Zhang, N. Kawazoe, G. Chen, Fabrication of highly crosslinked gelatin hydrogel and its influence on chondrocyte proliferation and phenotype, Polymers. 9(8) (2017).
[66] I. Caron, F. Rossi, S. Papa, R. Aloe, M. Sculco, E. Mauri, A. Sacchetti, E. Erba, N. Panini, V. Parazzi, M. Barilani, G. Forloni, G. Perale, L. Lazzari, P. Veglianese, A new three dimensional biomimetic hydrogel to deliver factors secreted by human mesenchymal stem cells in spinal cord injury, Biomaterials. 75 (2016) 135-147.
[67] A. Ziegler, L. Gonzalez, A. Blikslager, Large animal models: The key to translational discovery in digestive disease research, Cellular and molecular gastroenterology and hepatology. 2(6) (2016) 716-724.
[68] J.C. Fleming, M.D. Norenberg, D.A. Ramsay, G.A. Dekaban, A.E. Marcillo, A.D. Saenz, M. Pasquale-Styles, W.D. Dietrich, L.C. Weaver, The cellular inflammatory response in human spinal cords after injury, Brain : a journal of neurology. 129(Pt 12) (2006) 3249-69.
[69] J.R. Plemel, V. Wee Yong, D.P. Stirling, Immune modulatory therapies for spinal cord injury--past, present and future, Experimental neurology. 258 (2014) 91-104.
[70] K.A. Kigerl, J.C. Gensel, D.P. Ankeny, J.K. Alexander, D.J. Donnelly, P.G. Popovich, Identification of two distinct macrophage subsets with divergent effects causing either neurotoxicity or regeneration in the injured mouse spinal cord, The Journal of neuroscience : the official journal of the society for neuroscience. 29(43) (2009) 13435-44.
[71] H. Okano, Y. Ogawa, M. Nakamura, S. Kaneko, A. Iwanami, Y. Toyama, Transplantation of neural stem cells into the spinal cord after injury, Seminars in cell and developmental biology. 14(3) (2003) 191-198.
[72] J.E. Wells, R.J. Hurlbert, M.G. Fehlings, V.W. Yong, Neuroprotection by minocycline facilitates significant recovery from spinal cord injury in mice, Brain : a journal of neurology. 126(Pt 7) (2003) 1628-37.
[73] B.W. Festoff, S. Ameenuddin, P.M. Arnold, A. Wong, K.S. Santacruz, B.A. Citron, Minocycline neuroprotects, reduces microgliosis, and inhibits caspase protease expression early after spinal cord injury, Journal of neurochemistry. 97(5) (2006) 1314-26.
[74] A.D. Greenhalgh, S. David, Differences in the phagocytic response of microglia and peripheral macrophages after spinal cord injury and its effects on cell death, The Journal of neuroscience : the official journal of the society for neuroscience. 34(18) (2014) 6316-22.
[75] R. Shechter, M. Schwartz, Harnessing monocyte-derived macrophages to control central nervous system pathologies: no longer 'if' but 'how', The Journal of pathology. 229(2) (2013) 332-46.
[76] S. Papa, I. Vismara, A. Mariani, M. Barilani, S. Rimondo, M. De Paola, N. Panini, E. Erba, E. Mauri, F. Rossi, G. Forloni, L. Lazzari, P. Veglianese, Mesenchymal stem cells encapsulated into biomimetic hydrogel scaffold gradually release CCL2 chemokine in situ preserving cytoarchitecture and promoting functional recovery in spinal cord injury, Journal of controlled

782 release : official journal of the controlled release society. 278 (2018) 49-56.
783 [77] X. Zhou, X. He, Y. Ren, Function of microglia and macrophages in secondary damage after
784 spinal cord injury, Neural regeneration research. 9(20) (2014) 1787-95.
785

786

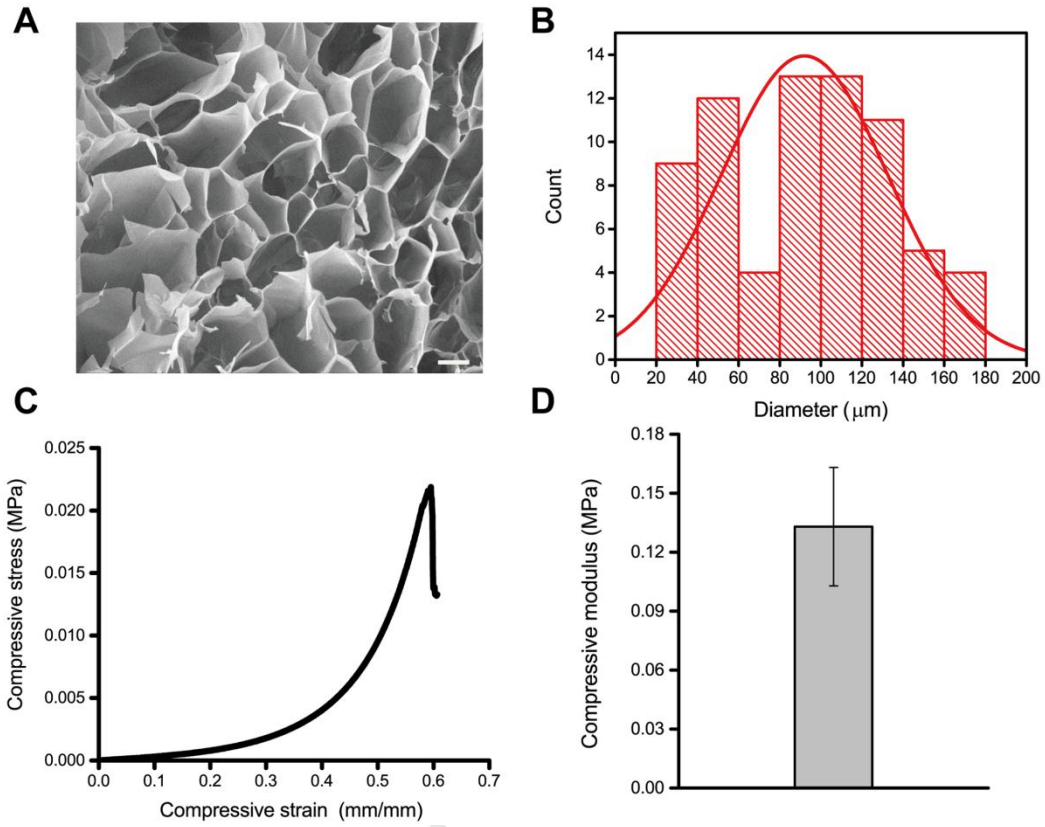

787

788 **Fig. 1.** Characterization of gelatin hydrogel. (A) SEM image of the gelatin hydrogel

789 (scale bar: 75 μm) and B) pore diameter distribution. (C) Compressive stress and (D)

790 modulus of the gelatin hydrogel.

791

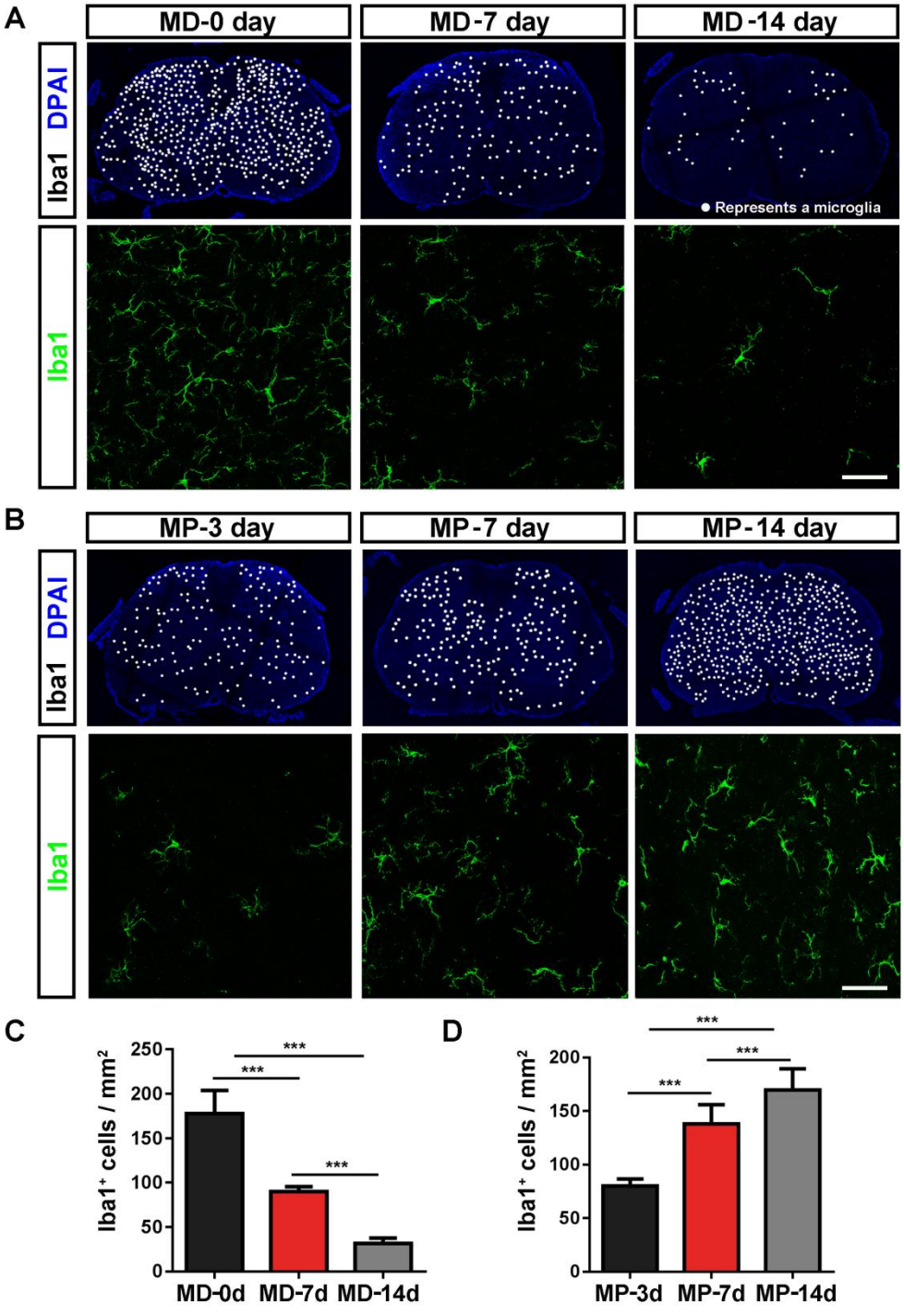

792

793 **Fig. 2.** Spinal cord microglial depletion (MD) and repopulation (MP) via the CSF1R

794 inhibitor, PLX3397. (A) Representative low and higher magnification images of

795 microglial depletion in the spinal cord after PLX3397 treatment for 0, 7 and 14 days.

796 (B) Representative low and higher magnification images show the density of

797 microglial repopulation at 3, 7 and 14 days after cessation of PLX3397 administration.

Mice were treated with PLX3397 for 14 days. (C) Quantification of the numbers of Iba1$^+$ cells per mm^2 at 0, 7 and 14 days after microglial depletion. (D) Quantification of the numbers of Iba1$^+$ cells per mm^2 at day 3, 7 and 14 after microglial repopulation. N=3 mice per group. Scale bars: 50 µm. *** p<0.001.

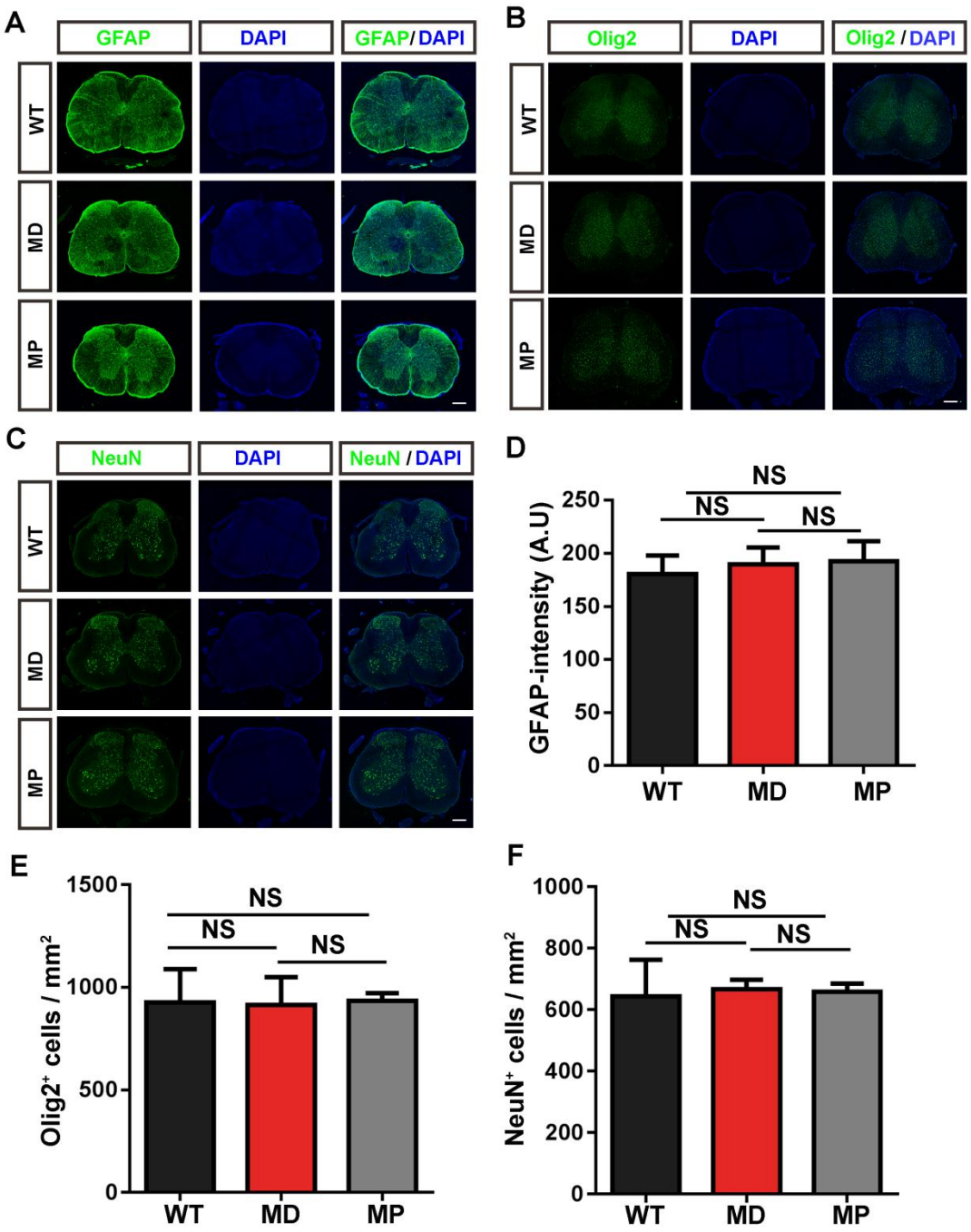

Fig. 3. Microglial depletion and repopulation do not affect other neural and glial cells in the spinal cord or the blood-spinal cord barrier. Representative images of (A) GFAP, (B) Olig2, and (C) NeuN immunofluorescence staining of the spinal cord from WT, MD and MP groups. Quantitative analysis of (E) the fluorescence density of astrocytes (GFAP) and (F) the cell density of neurons (NeuN) and (G)

809 oligodendrocytes (Olig2). N=3-4 mice per group. Scale bar: 500 μm. ^{NS} P>0.05.

810

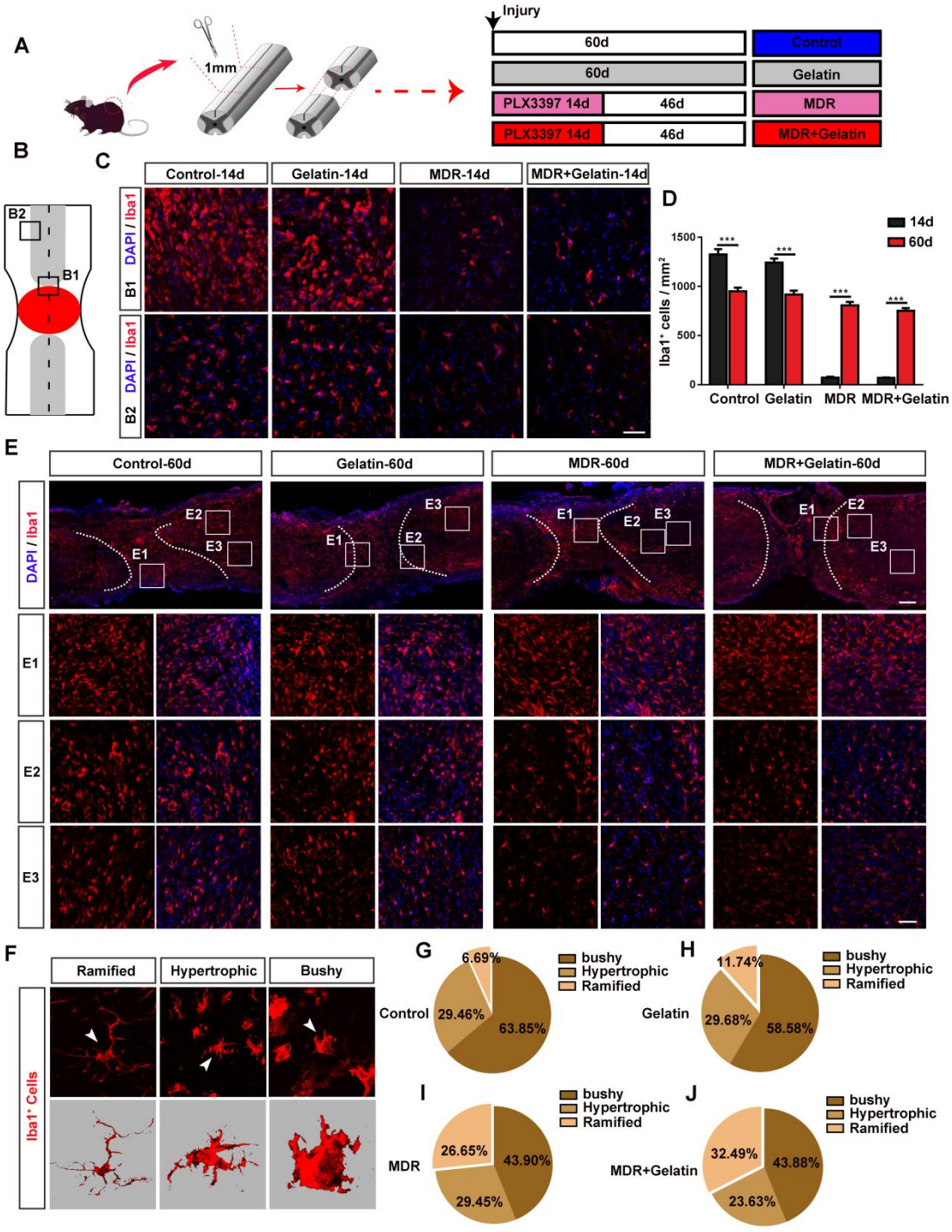

811

812 **Fig. 4.** Repopulating microglia/macrophages have a naïve state morphological
813 phenotype. (A) Diagram showing the SCI model and the experimental design. (B)
814 Cell sampling sites from injured spinal cord. (C) Representative images of the Iba1^{+}
815 cells and (D) quantification of the cell density of microglia/macrophages via Iba1

staining in the four experimental groups after treatment for 14 days. (E) Representative low and higher magnification images of $Iba1^+$ cells of Control, Gelatin, MD and MDR+Gelatin groups after SCI for 60 days. (F) The phenotype of resting and activated microglia/macrophages by Iba1 immunofluorescence staining. Quantification of the percentage of naïve, hypertrophic and bushy microglia/macrophage phenotypes in (G) Control, (H) Gelatin, (I) MD, and (J) MDR+Gelatin groups. (E1), (E2) and (E3) indicate Iba1-positive cells in the lesion center, adjacent and remote areas. N=3-4 mice per group. Scale bars represent 250 μm in first line of (E), and 50 μm in (C), (E1), (E2), and (E3). * $p<0.05$, *** $p<0.001$.

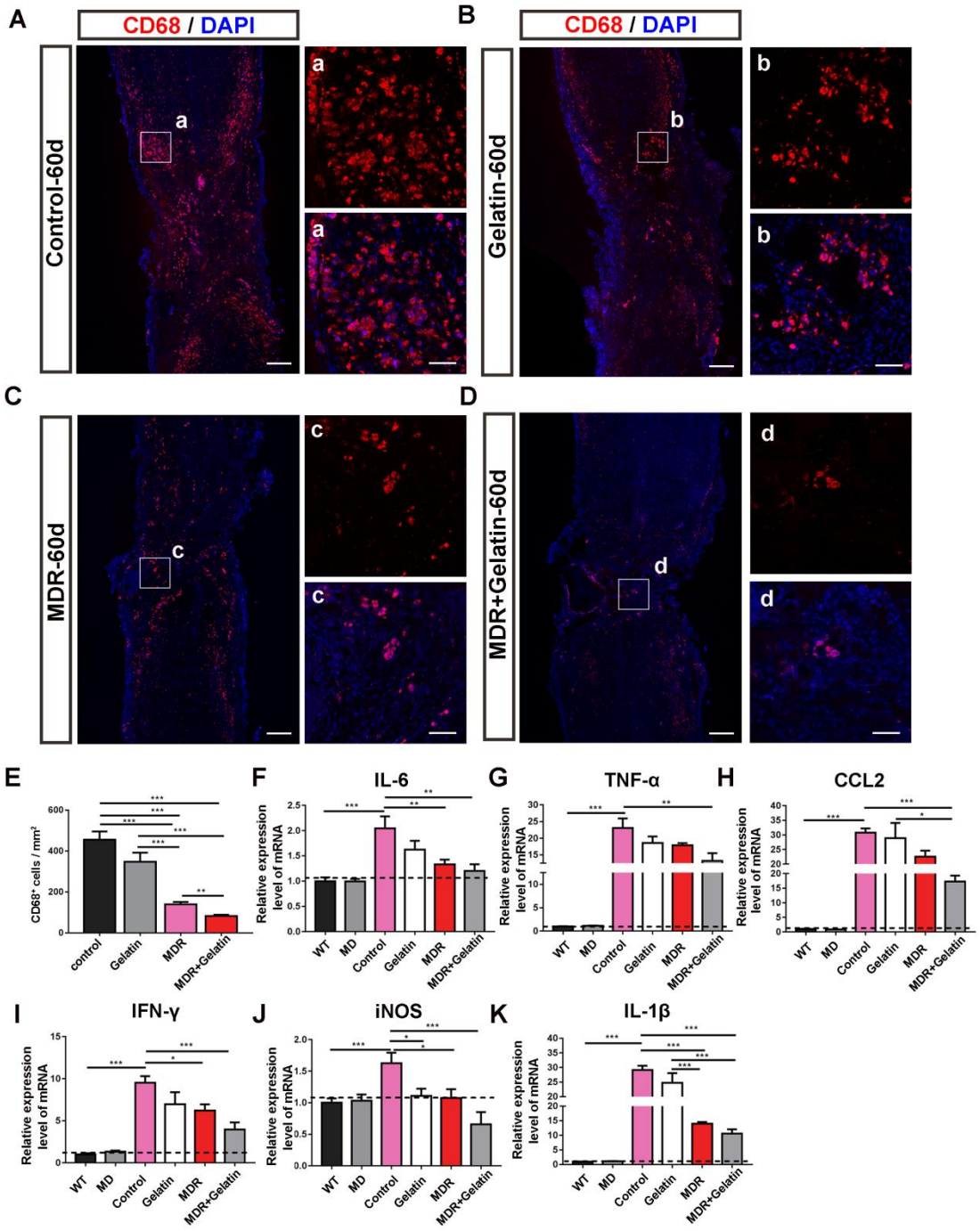

Fig. 5. Transplantation of gelatin hydrogel and replacement of activated with resting state microglia/macrophages effectively resolved inflammation. Representative images of CD68-positive cells in the (A) Control, (B) Gelatin, (C) MD and (D) MDR+Gelatin groups after SCI for 60 days. (E) Quantitation of (A-D) showing the number of $CD68^+$ cells per mm^2. N=3-4 mice per group. (F-K) mRNA levels of

pro-inflammatory factors, including IL6, TNFα, CCL2, IFNγ, iNOS, and IL1β in the four experimental groups at day 60 post-treatment. (a), (b), (c), (d) show higher magnification of CD68-positive cells. N=3-4 mice per group .Scale bar represents 250 µm in the lower magnification images of (A-D) and 50 µm in (a-d). * $p<0.05$ ** $p<0.01$ *** $p<0.001$.

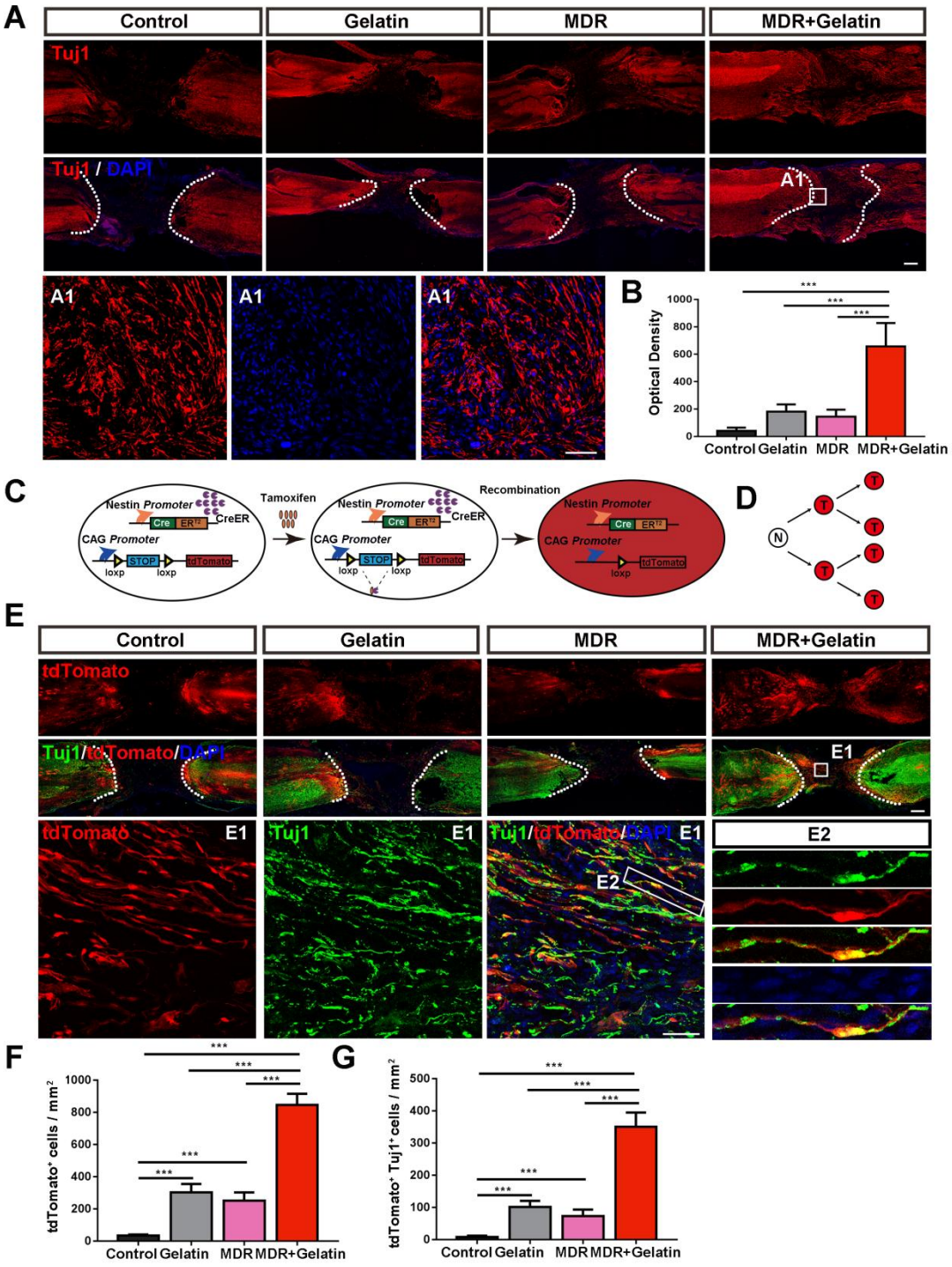

838

839 **Fig. 6.** Neural differentiation of NSPCs after transplantation of gelatin hydrogel and

840 resolution of microglia/macrophage mediated-inflammation. (A) Immunofluorescence

841 images and (B) the fluorescence density of Tuj1-positive neurons in Control, Gelatin,

842 MDR and MDR+Gelatin groups. A scheme representing the induction of (C) nestin+

843 cells and (D) their progenies in Nestin-CreER^{T2}; LSL-tdTomato mice injected with
844 tamoxifen. (E) Immunofluorescence images show that nestin+ NSPCs differentiated
845 to Tuj1-positive neurons in the MDR+Gelatin group. (F-G) Quantitative analysis of
846 tdTomato$^-$positive cells, as well as Tuj1 and tdTomato double-positive cells per mm^2
847 in the lesion area. (A1) shows Tuj1-positive cells in the lesion epicenter. (E1) and (E2)
848 show Tuj1, tdTomato double-positive cells in the lesion epicenter. N=3-4 mice per
849 group. Scale bars represent 250 μm in (A), (E) and 50 μm in (A1), (E1). *** $p<0.001$.
850

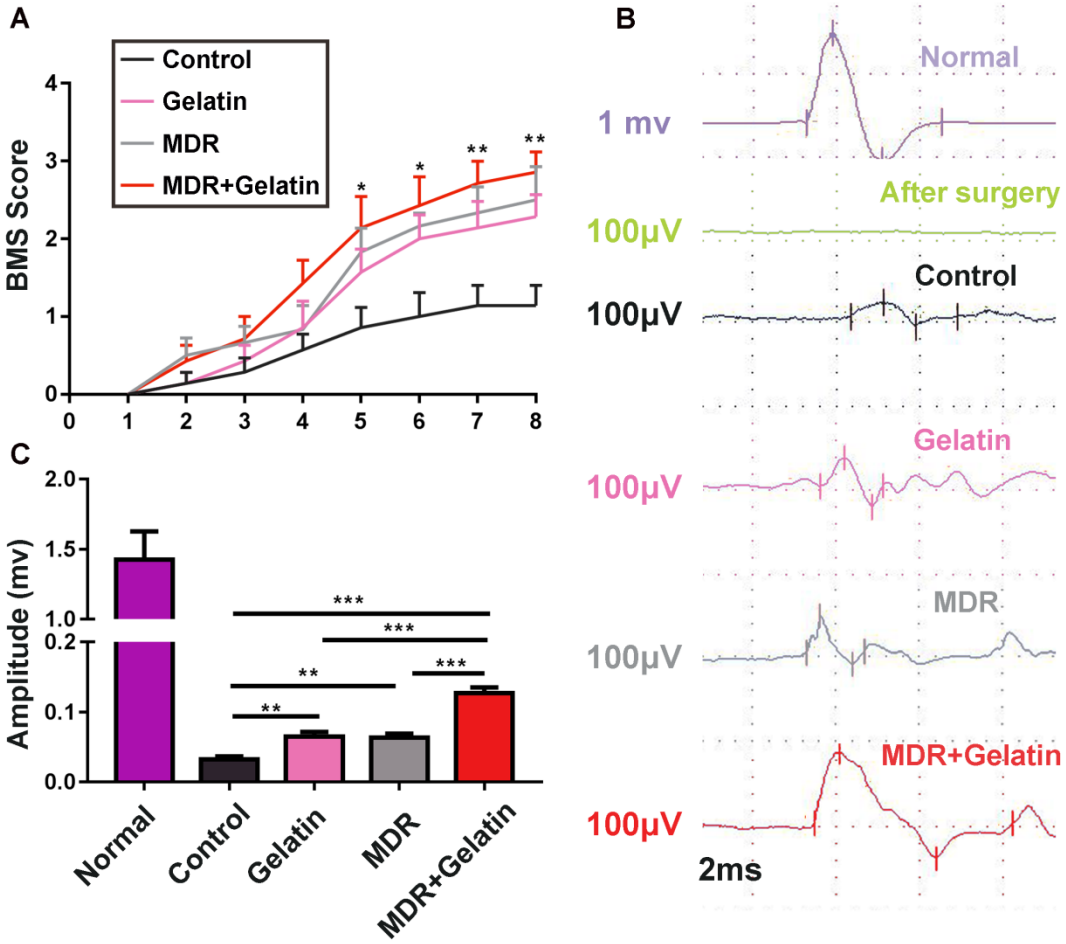

851

852 **Fig.7.** Transplantation of gelation combined with resolution of microglia/macrophage
853 mediated-inflammation promotes electrophysiological and functional motor recovery.
854 (A) Quantitative analysis of BMS scores in Control, Gelatin, MDR and MDR+Gelatin
855 groups after treatment for 1 to 8 weeks. (B) Representative images of motor evoked
856 potentials (MEPs) and (C) quantitation of amplitude in mice of each group after
857 treatment for 60 days. N=4-9 mice per group. * $p<0.05$ ** $p<0.01$ *** $p<0.001$.

858

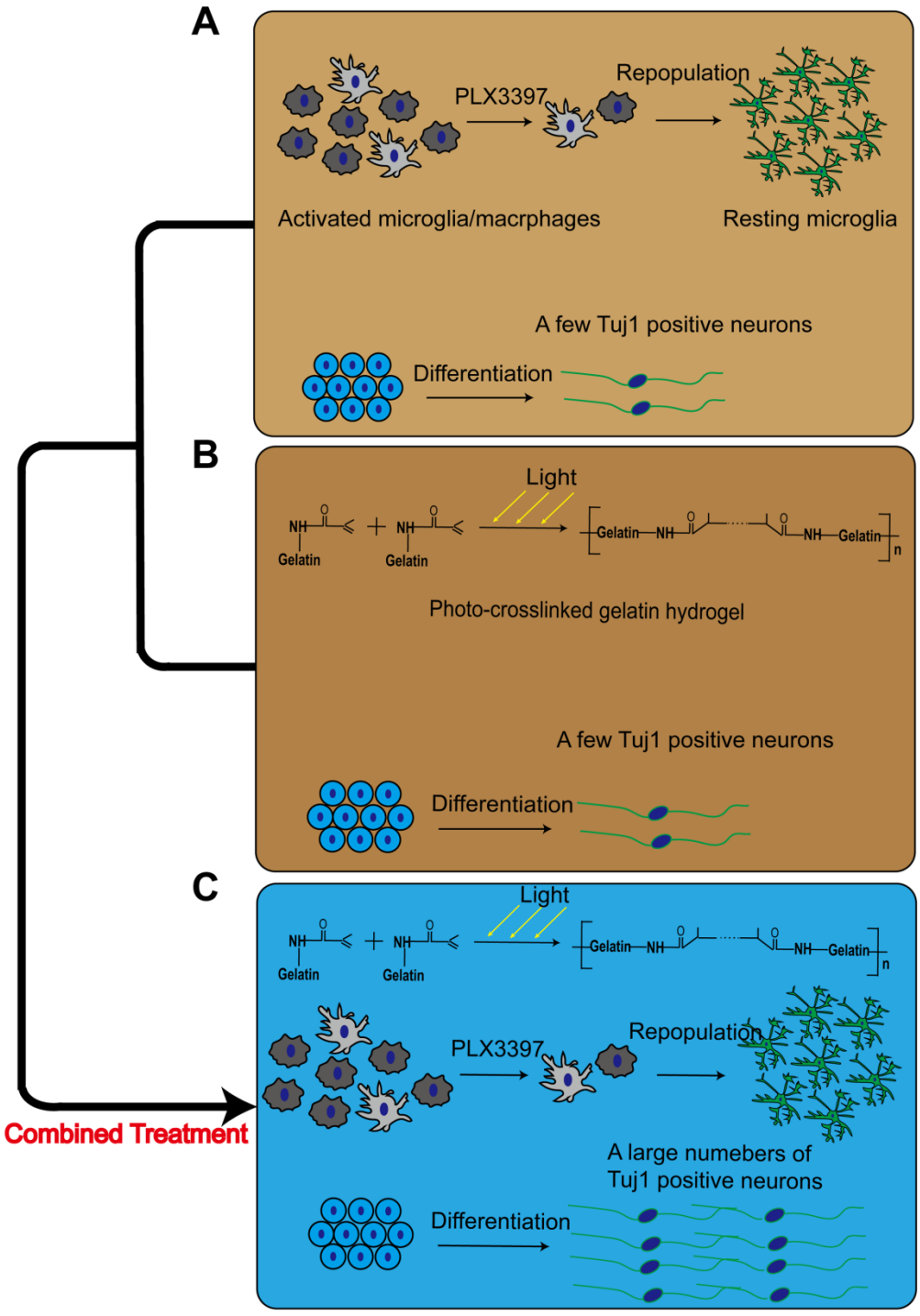

Fig. 8. (A-C) Schematic illustrations of photo-crosslinked gelatin hydrogel preparation and the resolution of microglia/macrophage mediated-inflammation by replacing activated microglia/macrophages after SCI.

Supporting Data

A Novel Hydrogel-based Treatment for Complete Transection Spinal Cord Injury Repair is Driven by Microglia/Macrophages Repopulation

Dezun Ma[a], Yannan Zhao[a], Lei Huang[b], Zhifeng Xiao[a], Bing Chen[a], Ya Shi[a], He Shen[b,*], Jianwu Dai[a,*]

[a]State Key Laboratory of Molecular Developmental Biology, Institute of Genetics and Developmental Biology, Chinese Academy of Sciences, Beijing 100101, P.R. China.

University of Chinese Academy of Sciences, Beijing, 100101, P.R. China

[b]Key Laboratory for Nano-Bio Interface Research, Division of Nanobiomedicine, Suzhou Institute of Nano-Tech and Nano-Bionics, Chinese Academy of Sciences, Suzhou 215123, China

Corresponding authors: Jianwu Dai, Email: jwdai@genetics.ac.cn

He Shen, Email: hshen2009@sinano.ac.cn

883 **Supplemental Figures**

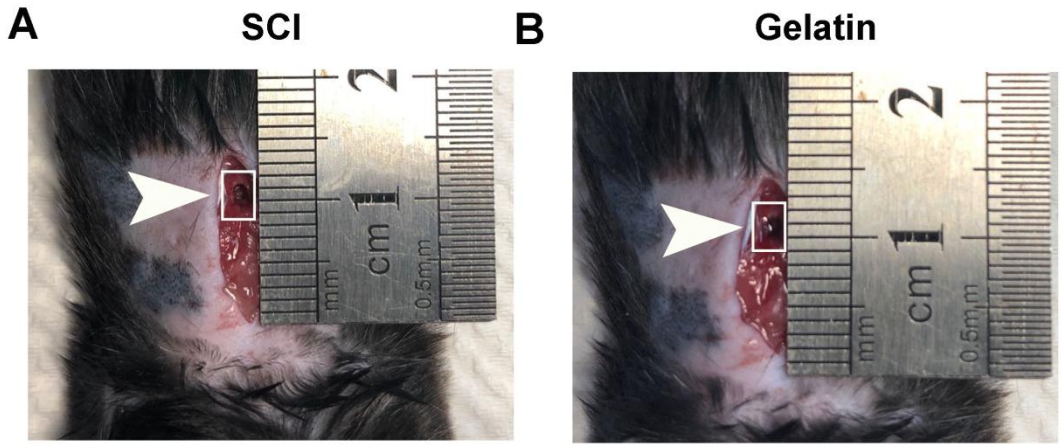

884

885 **Fig. S1.** Photo images of SCI and hydrogel transplantation. Arrowheads and white

886 frames indicate the injury sites.

887

888

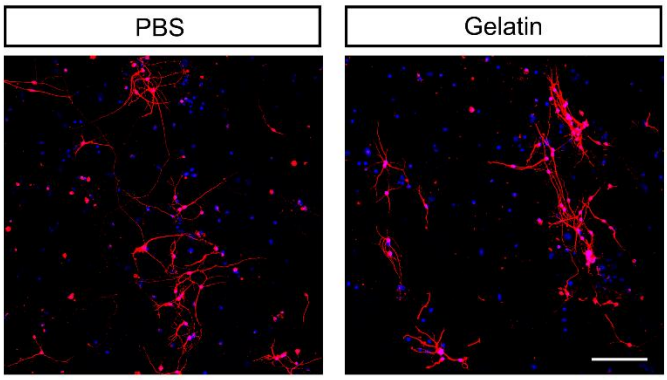

889

890 **Fig. S2.** Images of cells with PBS and gelatin hydrogel treatment for 7 days,

891 immunofluorescence stained with Tuj-1 (red) and DAPI (blue). Scale bar = 100 μm.

892

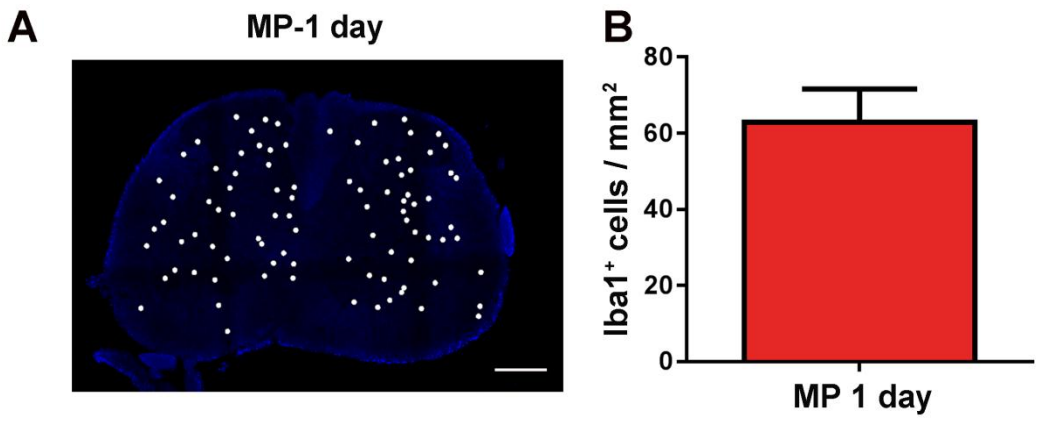

Fig. S3. Microglial repopulation at 1 day after stopping PLX3397 feeding for 14 days. (A) Representative images of microglial repopulation in the spinal cord at 1 day after cessation of PLX3397 administration. Each white dot represents a microglia. (B) Quantification of the numbers of Iba1+ cells per mm^2 at 1 days after microglial repopulation, respectively. N = 3 mice per group. Scale bars: 250 μm.

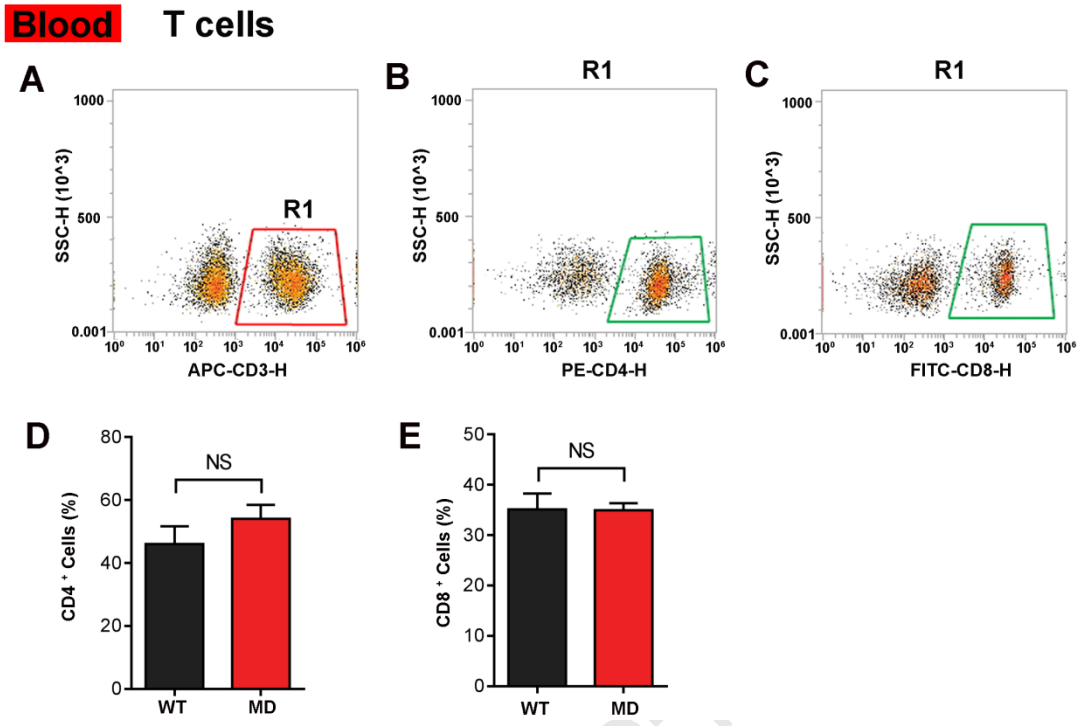

901

902 **Fig. S4.** Microglial depletion after PLX3397 treatment produces no obvious

903 differences in blood T cells. Identification of (A) CD3, (B) CD4 and (C) CD8 T cell

904 subsets via a gating strategy. Quantitative analysis of the percentage of (D) CD4 and

905 (E) CD8 positive cells. N=3 mice per group. ^{NS} P>0.05.

906

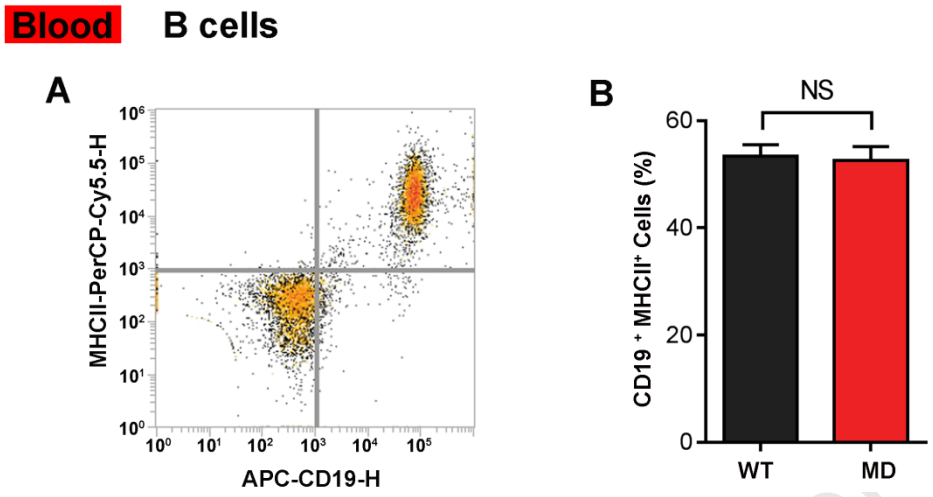

907

908 **Fig. S5.** Microglial depletion after PLX3397 treatment does not alter blood B cells. (A)

909 Identification of CD19 and MHCII cell subsets via a gating strategy. (B) Quantitative

910 analysis of the percentage of CD19, MHCII double-positive B cells. N=3 mice per

911 group. ^{NS} P>0.05.

912

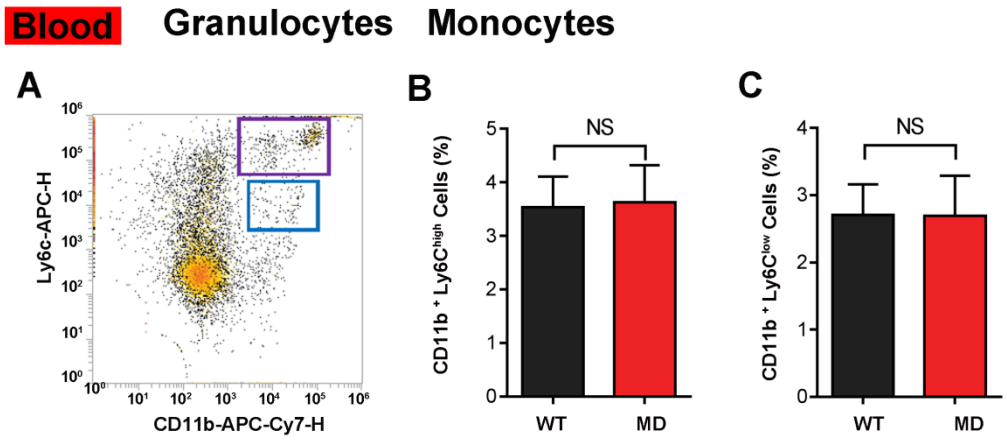

913

914 **Fig. S6.** Microglial depletion after PLX3397 treatment does not change blood

915 granulocytes or monocytes. (A) Identification of granulocyte and monocyte subsets

916 via a gating strategy. Quantitative analysis of the percentage of (B) $CD11b^{+}$ $Ly6C^{high}$

917 and (C) $CD11b^{+}$ $Ly6C^{low}$ cells. N=3 mice per group. ^{NS} P>0.05.

918

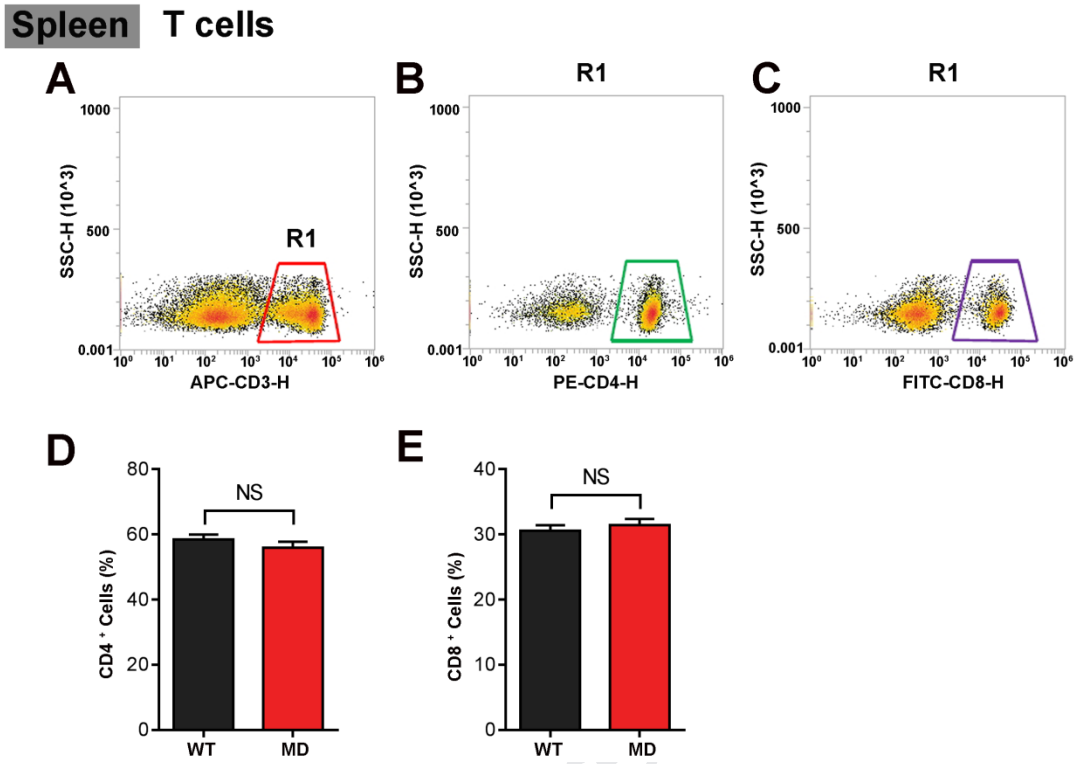

Fig. S7. Microglial depletion after PLX3397 treatment does not change spleen T cells. Identification of (A) CD3, (B) CD4 and (C) CD8 T cell subsets via a gating strategy. Quantitative analysis of the percentage of (D) CD4 and (E) CD8-positive cells. N=3 mice per group. ^{NS} P>0.05.

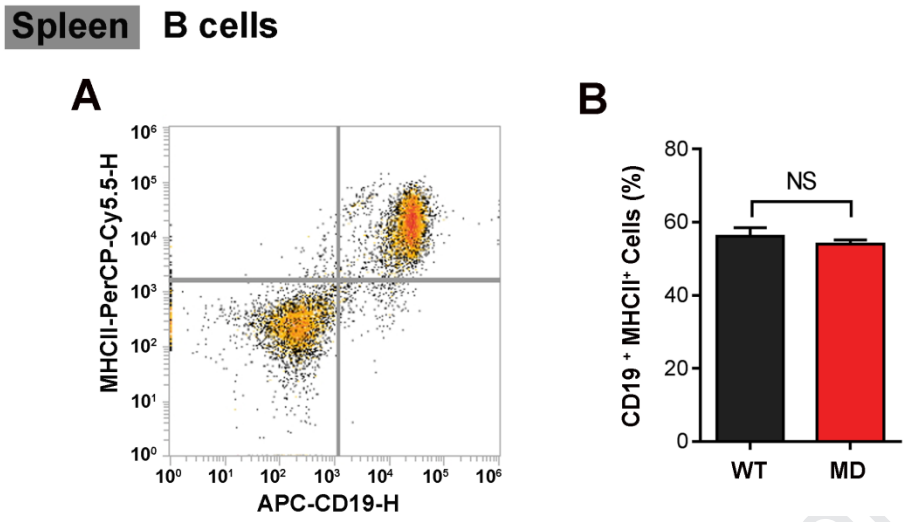

Fig. S8. Microglial depletion after PLX3397 treatment does not alter spleen B cells. (A) Identification of CD19 and MHCII cell subsets via a gating strategy. (B) Quantitative analysis of the percentage of CD19, MHCII double-positive B cells. N=3 mice per group. ^{NS} P>0.05.

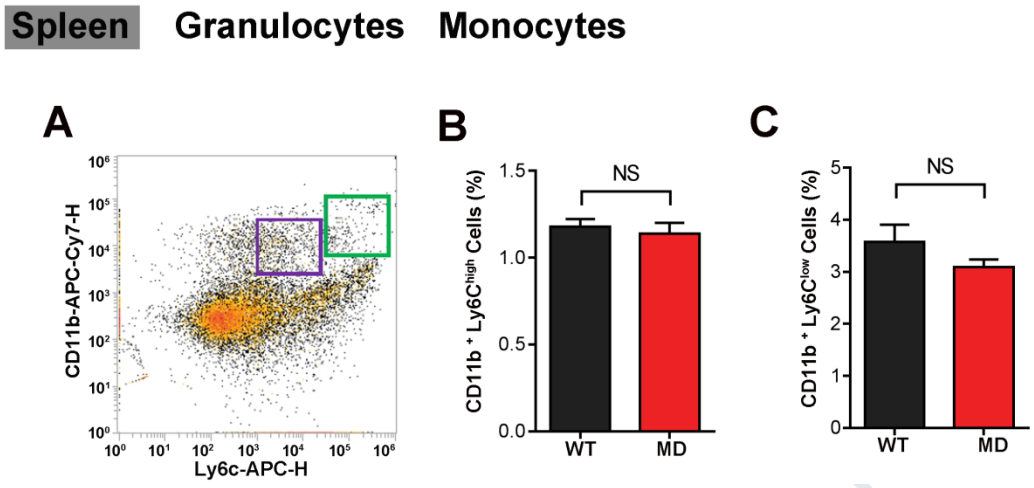

931

932 **Fig. S9.** Microglia depletion after PLX3397 treatment does not change spleen

933 granulocytes or monocytes. (A) Identification of granulocyte and monocyte subsets

934 via a gating strategy. Quantitative analysis of the percentage of (B) $CD11b^{+}$ $Ly6C^{high}$

935 and (C) $CD11b^{+}$ $Ly6C^{low}$ cells. N=3 mice per group. ^{NS} P>0.05.

936

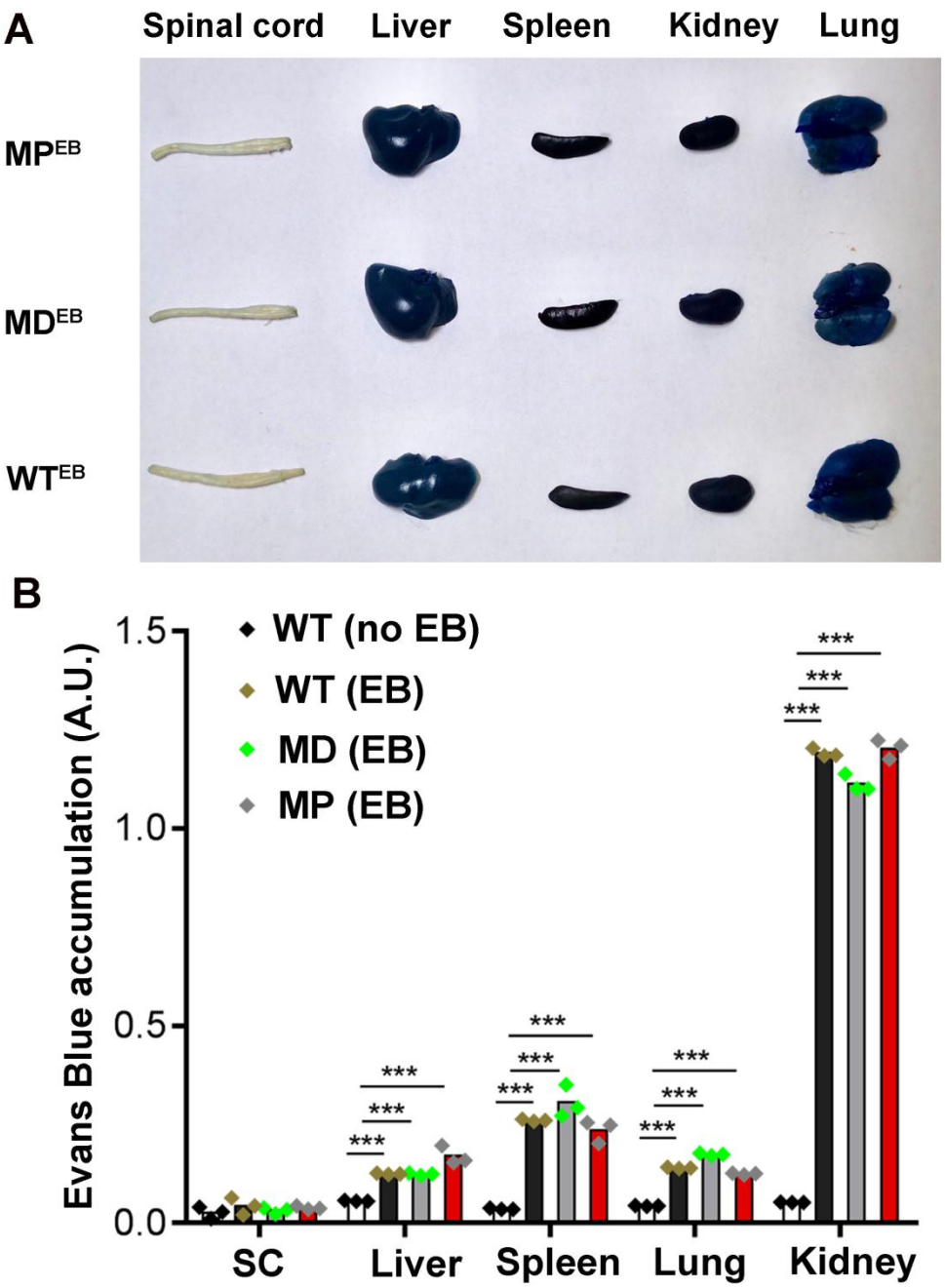

937

938 **Fig. S10.** (A) Representative images showing that microglia depletion does not

939 damage the integrity of the blood-spinal cord barrier. N=3 mice per group. (B)

940 Quantitative absorption of Evans blue (EB) in the spinal cord (SC), liver, spleen, lung

941 and kidney from WT, MD and MP groups.

942

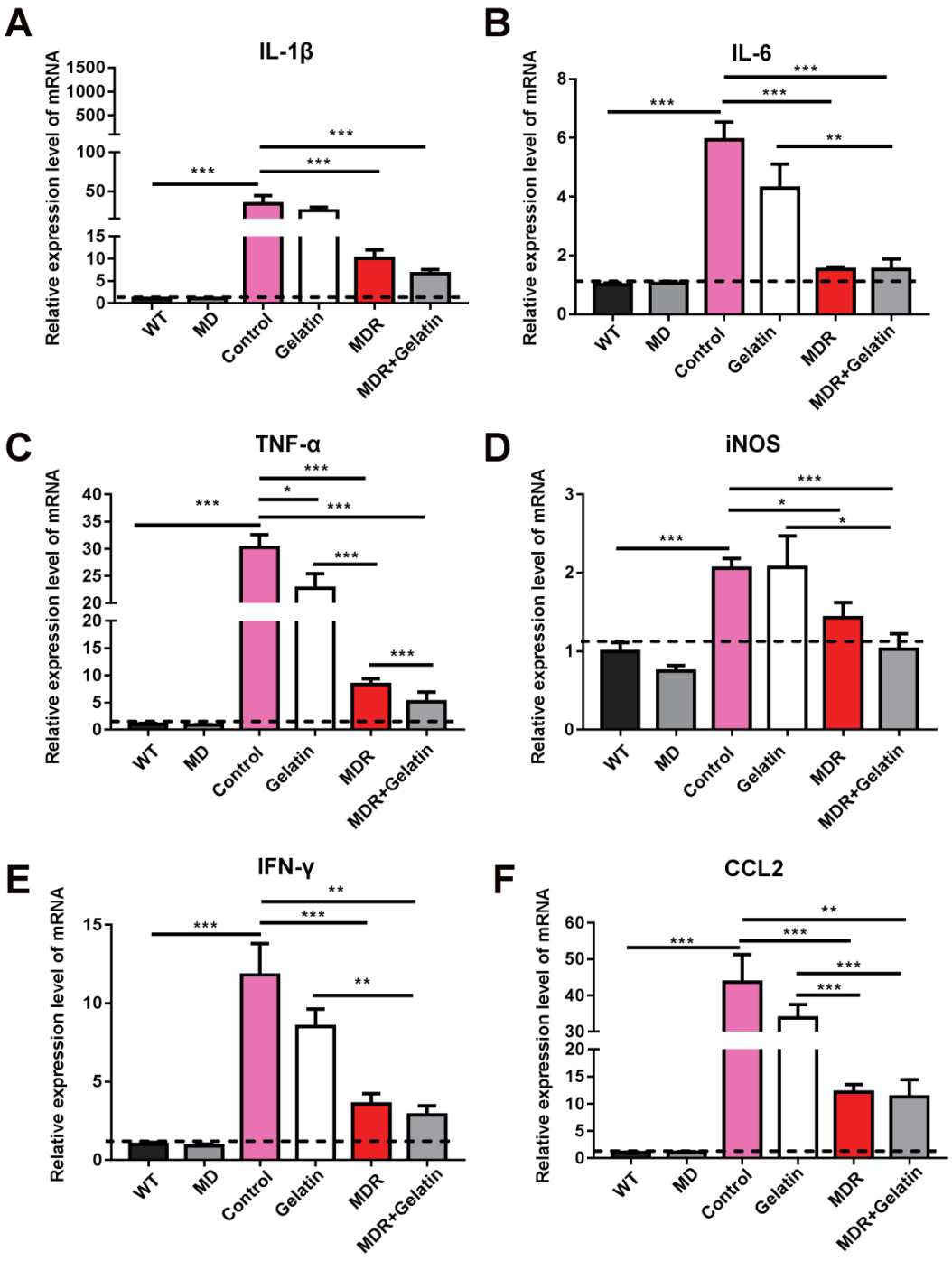

943

944 **Fig. S11.** Microglia/macrophage depletion after PLX3397 treatment for 14 days

945 reduces the secretion of pro-inflammatory factors. The mRNA levels of

946 pro-inflammatory factors (A) IL1β, (B) IL6, (C) TNFα, (D) iNOS, (E) IFNγ and (F)

947 CCL2 at day 14 post-surgery. N=3-4 mice per group. * $p<0.05$ ** $p<0.01$ ***

948 $p<0.001$.

949 **Supplemental Table**

950 **Table S1**. The primers for Real-Time Quantitative PCR

Gene	Sequence
IL1β	CTCCATGAGCTTTGTACAAGG (Forward)
	GGGGTTGACCATGTAGTCGT (Reverse)
IL6	AAGAAAGACAAAGCCAGAGTC (Forward)
	CACAAACTGATATGCTTAGGC (Reverse)
TNFα	TCAGCCTCTTCTCATTCCTGC (Forward)
	TTGGTGGTTTGCTACGACGTG (Reverse)
iNOS	GACGAGACGGATAGGCAGAG (Forward)
	CACATGCAAGGAAGGGAACT (Reverse)
IFNγ	ATCAGGCCATCAGCAACAA (Forward)
	ACCTGTGGGTTGTTGACCTC (Reverse)
CCL2	TAAAAACCTGGATCGGAACCAAA (Forward)
	GCATTAGCTTCAGATTTACGGGT (Reverse)

951

Declaration of interests

☒ The authors declare that they have no known competing financial interests or personal relationships that could have appeared to influence the work reported in this paper.

☐The authors declare the following financial interests/personal relationships which may be considered as potential competing interests: